Justus-Liebig-University Gießen
Faculty 09 - Agricultural Sciences, Nutritional Sciences and Environmental Management
Department of Landscape Ecology and Resources Management

Simulating potential yield if industry is disabled: Applying a generalized linear modelling approach to major food crops

Master Thesis in Environmental Sciences

Submitted by: Jessica Mörsdorf
Matriculation Number: 3000994
Supervisors: Florian Ulrich Jehn
Prof. Dr. Lutz Breuer
Submission date: 23rd of October 2021

Abstract

Modern civilization is highly dependent on industrial agriculture. Industrial agriculture in turn has become an increasingly complex and globally interconnected system whose historically unprecedented productivity relies strongly on external energy inputs in the shape of machinery, mineral fertilizers, and pesticides. It leaves the system vulnerable to disruptions of industrial production and international trade. Several scenarios have the potential to damage electrical infrastructure on a global scale, including electromagnetic bursts caused by solar storms or the detonation of nuclear warheads in the higher atmosphere, as well as a globally coordinated cyber-attack. The current COVID-19 pandemic has highlighted the importance of crisis preparation and the establishment of more resilient systems. To improve preparation for high-stake risk scenarios their impact especially on critical supply systems must be better understood. To further the understanding of consequences for the global food production this work aims to estimate the effect the global inhibition of industrial production could have on the crop yields of maize, rice, soybean, and wheat.

A generalized linear model with a gamma distribution was calibrated on current crop-specific gridded global yield datasets at five arcmin resolution. Gridded datasets on the temperature regime, the moisture regime, soil characteristics, nitrogen, phosphorus and pesticide application rates, the fraction of irrigated area and a proxy to determine whether farm activities are mechanized were chosen as explanatory variables. The model was then used to predict crop yields in two phases following a global catastrophe which inhibits the usage of any electric services. Phase 1 reflects conditions in the year immediately after the catastrophe, assuming the existence of fertilizer, pesticides, and fuel stocks. In phase 2 all stocks are used up and fertilizer, pesticides and fuel are not available anymore.

While the fit varies dependent on the crop, the model agrees well with the data based on McFadden's ρ^2 (maize: 0.45, rice: 0.41, soybean: 0.34, wheat: 0.38). The predictions showed a reduction in yield of 10-30% in phase 1 and between 34 and 43% in phase 2. Overall Europe, North and South America and large parts of India, China and Indonesia are projected to face major yield reductions of up to 95% while most African countries are scarcely affected.

The findings clearly indicate hotspot regions which align with the level of industrialization of agriculture. Further, it is shown that the yield reduction is likely

to be substantial, especially in industrialized countries. The analysis also provides insights on major factors influencing crop yield under losing industry circumstances. Due to data unavailability some crucial factors could not be included in the model, but their qualitative discussion leads to the conclusion that the presented results can be considered optimistic, and that further research is needed to quantify the impact of the omitted aspects.

Zusammenfassung

Die moderne Zivilisation ist in hohem Maße von der industriellen Landwirtschaft abhängig. Die industrielle Landwirtschaft wiederum ist zu einem immer komplexeren und global vernetzten System geworden, dessen historisch beispiellose Produktivität stark von externen Energiezufuhren in Form von Maschinen, Mineraldünger und Pestiziden abhängt. Dadurch wird das System anfällig für Störungen der industriellen Produktion und des internationalen Handels. Mehrere Szenarien haben das Potenzial, die elektrische Infrastruktur auf globaler Ebene zu beschädigen, darunter starke elektromagnetische Impulse, welche durch Sonnenstürme oder die Detonation von Atomsprengköpfen in der höheren Atmosphäre ausgelöst werden können, sowie ein global koordinierter Cyberangriff. Die aktuelle COVID-19-Pandemie hat gezeigt, wie wichtig die Krisenvorbereitung und die Einrichtung widerstandsfähigerer Systeme sind. Um die Vorbereitung auf Szenarien mit hohem Risiko zu verbessern, müssen deren Auswirkungen, insbesondere auf kritische Versorgungssysteme, besser verstanden werden. Das Ziel dieser Arbeit ist es, die Auswirkungen abzuschätzen, die eine weltweite Einschränkung der industriellen Produktion auf die Ernteerträge von Mais, Reis, Sojabohnen und Weizen haben könnte und somit zum besseren Verständnis der Folgen für die weltweite Nahrungsmittelproduktion beizutragen.

Es wurde ein verallgemeinertes lineares Modell basierend auf einer Gamma-Verteilung an aktuellen kulturspezifischen globalen Ertragsdatensätzen mit einer Auflösung von fünf Bogenminuten kalibriert. Als erklärende Variablen wurden georeferenzierte Datensätze über das Temperaturregime, das Feuchtigkeitsregime, die Bodeneigenschaften, die Stickstoff-, Phosphor- und Pestizidausbringungsraten, den Anteil der bewässerten Fläche und einen Proxy zur Bestimmung des Mechanisierungsgrads der landwirtschaftlichen Tätigkeiten gewählt. Das Modell wurde dann verwendet, um die Ernteerträge in zwei Phasen nach einer globalen Katastrophe vorherzusagen, die die Nutzung jeglicher elektrischen Infrastruktur verhindert. Phase 1 spiegelt die Bedingungen im Jahr unmittelbar nach der Katastrophe wider, wobei davon ausgegangen wird, dass Düngemittel-, Pestizid- und Kraftstoffvorräte vorhanden sind. In Phase 2 sind alle Vorräte aufgebraucht, und Düngemittel, Pestizide und Treibstoff sind nicht mehr verfügbar.

Obwohl der Fit je nach Kultur variiert, stimmt das Modell auf der Grundlage des ρ^2 von McFadden gut mit den Daten überein (Mais: 0,45, Reis: 0,41, Sojabohnen:

0,34, Weizen: 0,38). Die Vorhersagen zeigten eine Ertragsminderung von 10-30 % in Phase 1 und zwischen 34 und 43 % in Phase 2. Insgesamt werden für Europa, Nord- und Südamerika und große Teile Indiens, Chinas und Indonesiens erhebliche Ertragseinbußen von bis zu 95 % prognostiziert, während die meisten afrikanischen Länder kaum betroffen sind.

Die Ergebnisse weisen eindeutig auf Hotspot-Regionen hin, die mit dem Grad der Industrialisierung der Landwirtschaft übereinstimmen. Außerdem wird gezeigt, dass die Ertragseinbußen voraussichtlich besonders in den Industrieländern erheblich sein werden. Die Analyse gibt auch Aufschluss über die wichtigsten Faktoren, die die Ernteerträge unter den Bedingungen eines industriellen Stillstandes beeinflussen. Aufgrund der Nichtverfügbarkeit von Daten konnten einige entscheidende Faktoren nicht in das Modell aufgenommen werden. Jedoch führt die qualitative Diskussion dieser Faktoren zu der Schlussfolgerung, dass die vorgestellten Ergebnisse als optimistisch angesehen werden können und dass weitere Forschung erforderlich ist, um die Effekte der ausgelassenen Aspekte zu quantifizieren.

Acknowledgements

I want to thank my supervisor, Florian Ulrich Jehn, for providing the opportunity to get engaged in the Global Catastrophic Risks research and guiding my work process. I am grateful for your motivational words and that I could reach out to you anytime (even when you were on vacation). Thank you, as well to the second corrector of my thesis, Prof. Dr. Lutz Breuer, for your advice and your constructive feedback

I am fortunate to have been a part of the ALLFED team throughout my thesis research. I am very grateful for all the support and valuable feedback I received from my ALLFED colleagues. Thank you, Dr. David Denkenberger, for your expertise and thoughtful comments and thank you Mike Hinge for the long and interesting discussions on agricultural history (and anything that sparked our interest along the way for that matter). I want to thank Morgan Rivers in particular. Thank you for your invaluable assistance with the programming part of this thesis and for your patience in hourlong calls on methodological and technological issues. Computers can be headstrong, and I couldn't have navigated all the pitfalls without you.

I would like to thank Dr. Christina Ramsenthaler and Dr. Ruslan Krenzler for much needed guidance in statistical questions.

A special thank you goes to Hans Hartwig Lützow and the Untermühlbachhof. Thank you for letting me stay overnight and taking the time to answer all my questions about low tech agricultural techniques and the work with draft animals.

I'm grateful for the public library in Bad Wurzach and its staff for providing a change of scene and the opportunity to spend many hours in the beautiful historical building.

Thank you to my bosses, Katja Filippenko and Dr. Stéphanie Domptail for being amazing and inspiring women who excel in their respective fields. Thank you both for being a source of inspiration and for your lenience and flexibility when the thesis work made days seem way too short.

Finally, thank you to my family and my partner. Any attempt to value your part in this thesis would fall short. Thank you for believing in me when I didn't.

Table of Contents

I. Index of Tables

II. Index of abbreviations

(Global) Agroecological Zones	(G)AEZ
Alliance to Feed the Earth in Disaster	ALLFED
American Standard Code for Information Interchange	ASCII
Coronal Mass Ejection	CME
Coronavirus disease 2019	COVID-19
Decision Support System for Agrotechnology Transfer	DSSAT
(High Altitude) Electromagnetic Pulse	(H)EMP
Food and Agriculture Organization	FAO
Food and Agriculture Organization Statistics	FAOSTAT
Generalized Linear Model	GLM
Genetically Modified	GM
Global Catastrophic Risks	GCR
Global Livestock Impact Mapping System	GLIMS
Large Power Transformer	LPT
Intergovernmental Panel on Climate Change	IPCC
International Energy Agency	IEA
International Fertilizer Association	IFA
Loss of industry/industrial civilization; Losing industry	LoI
Pesticide National Synthesis Project	PNSP
Quantum Geographic Information System	QGIS
Root Mean Gamma Deviance	RMGD
Spatial Production Allocation Model	SPAM
United States Geological Survey	USGS
Variance Inflation Factor	VIF

III. List of Figures

1 Introduction

The development of agriculture was a major turning point in human history. By offering a stable food source throughout the year, agriculture facilitated the emergence of complex societies all around the globe (Miedaner, 2005; Smil, 2017). Agricultural practices developed simultaneously in multiple different cultures, but yields were low and crop production entailed many hours of hard labor: despite its merits, food production in agricultural societies still required the involvement of the better part of the population to feed everyone.

It wasn't until the rise of modern technology which allowed the harnessing of energy from fossil fuels and its introduction into agriculture in the shape of machinery, artificial fertilizer, and pesticides during the twentieth century that populations in the billions could develop. This stark increase was supported by an expansion of cropland by 40% (Smil, 2017, p. 311), by substantially decreasing the number of human work hours required to produce one ton of grain from 30h/t in 1800 to just 90 min/t in 2000 (Smil, 2017, p. 307) and by at least quadrupling staple crops yields since before the Industrial Revolution (Ritchie & Roser, 2013). By freeing up energy for activities besides food production the steady decline of the share of agricultural workers in the workforce to just 27% globally in 2019 (World Bank, 2021) played a crucial role in facilitating the current level of complexity in society.

But the rapid agricultural and societal development has severe consequences, like the devastating environmental effects (Flynn, 1999; Kopittke, Menzies, Wang, McKenna, & Lombi, 2019; Lee & Nielsen, 1987; Naeem, Ansari, & Gill, 2020; Sánchez-Bayo & Wyckhuys, 2019) or the challenges related to climate change (Dempewolf et al., 2014; Myers et al., 2017; Vermeulen, Campbell, & Ingram, 2012), and the decreasing margins of yield increase (Alston & Pardey, 2014; M. K. van Ittersum et al., 2013). One aspect, however, has been underreported in the literature while being not less crucial: The advances of modern technology in agriculture have also resulted in a strong dependence of food security on global trade and industrial infrastructure (Neff, Parker, Kirschenmann, Tinch, & Lawrence, 2011; Smil, 2017, p. 306). This makes the system vulnerable to scenarios in which industrial infrastructure is disrupted. Especially on a global scale the impact can be disastrous. The current COVID-19 pandemic has demonstrated that events deemed highly unlikely can still occur at any given time and has exposed the

lack of preparedness in most countries (Brozus & Stiftung Wissenschaft und Politik, 2020; Liu, Lauta, & Maas, 2020). Therefore, it is imperative that preventive action is taken because as Nick Bostrom states in an existential catastrophe “there is no opportunity to learn from errors.” To better gauge the impact the inhibition of industrial infrastructure can have, this work seeks to present a first estimate of the expectable changes in agricultural yield in the case of a loss of industry. Based on a multiple regression analysis on spatial data, yields for a worst-case scenario are predicted to understand the effects of a disturbance of industrial infrastructure on modern agriculture.

2 Background

2.1 Global Catastrophic Risks

The term Global Catastrophic Risks (GCR) has been introduced by Nick Bostrom. He loosely defines it as "a risk that might have the potential to inflict serious damage to human well-being on a global scale" (Bostrom & Ćirković, 2008b). To more clearly delimit what serious damage on a global scale might entail, Bostrom and Ćirković (2008b) propose that an event causing ten million fatalities or ten trillion dollars worth of economic damage qualifies as a global catastrophe. Depending on the current estimates of economic losses, the COVID-19 pandemic ranges close or even already surpassed the ten trillion-dollar threshold (Cutler & Summers, 2020; Lenzen et al., 2020; Park et al., 2020; United Nations Conference on Trade and Development [UNCTAD], 2021). However, a global pandemic is just one of many different GCR scenarios compiled in Bostrom and Ćirković's book (2008a) and in other GCR research. Possible causes natural risks such as super-volcanoes, comets, and asteroid impacts, risks from unintended consequences like climate change, pandemics, or artificial intelligence, and risks from malintent such as nuclear wars or biotechnological attacks. Further it is cautioned that new risks emerge as technology develops and that potential risks might be undetected or misjudged due to biases or lack of sufficient knowledge to understand the impact (Sandberg, 2018; Wiener, 2016; Yudkowsky, 2008).

In the light of the sheer number of possible scenarios, classification schemes have been proposed to manage the scope. In addition, many experts (Avin et al., 2018; S. Baum & Barrett, 2017; see e.g. Bostrom & Ćirković, 2008a) in the field point out that in terms of risk assessment GCRs should be considered as a combined threat rather than individual scenarios because interactions between scenarios can increase the magnitude of a catastrophe's impact and the nature of the catastrophe which is first to strike remains uncertain. Bostrom and Ćirković (2008b) present a taxonomy along the dimensions of scope (personal to transgenerational), intensity (imperceptible to terminal), and probability. In choosing these dimensions, Bostrom and Ćirković (2008b) place GCRs in a scale encompassing a continuum from "normal" to existential risks, with the GCRs being demarcated via their large scope and high intensity. Existential risks are presented as a subclass of GCRs which are so severe that they lead to human extinction.

Avin et al. (2018) take a different approach as they emphasize the importance of "[…] a methodology for compiling a comprehensive, interdisciplinary view of severe global catastrophic risks." In accordance with this goal, Avin et al. (2018) focus more strongly than Bostrom and Ćirković (2008b) on qualitative rather than quantitative characteristics of GCR scenarios. The classification proposes to inquire which critical system is affected by the scenario, by which global mechanisms it uses to spread, and which prevention and mitigation fragilities exist (Avin et al., 2018).

This approach concentrates to a greater extent on systemic consequences of GCRs but S. D. Baum, Denkenberger, Pearce, Robock, and Winkler (2015) and others (e.g. Sandberg, 2018) have highlighted the importance of one critical system for human survival: the food production system. They argue that it is affected by most GCRs (Avin et al., 2018) and that it constitutes the mechanism by which many GCRs endanger humanity's survival, namely by compromising agricultural production to the point of mass starvation. Based on the importance of the food system, the Alliance to Feed the Earth in Disasters (ALLFED, 2021) provides a framework for GCRs centered around the consequences for the global food production. The framework will be used to contextualize the scenarios investigated in this thesis. Figure 1 shows a scale in terms of percent of damage to the food production system and specifies five categories of disasters which vary in the degree of damage inflicted on the food production system. The lower and upper categories are presented as out of scope for global catastrophic food loss scenarios

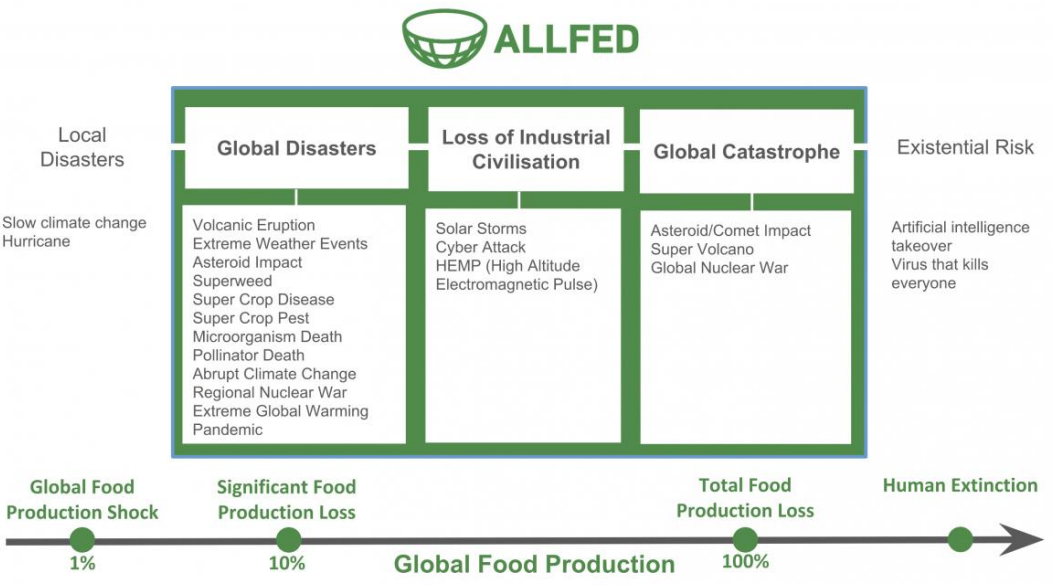

Figure 1: Food Production Loss Scenarios (ALLFED, 2021)

because local disasters don't qualify as global catastrophes in terms of scope and existential risks are assumed to result in catastrophes severe enough to cause extinction faster than mass starvation. This leaves three categories of risks with severe consequences for the food production system which warrant closer inspection. Global disasters are expected to result in severe damage, causing between a three to thirty percent reduction in the food production capacity but without primary consequences for the structure of the agricultural system. Loss of industrial civilization (LoI) scenarios and global catastrophic scenarios have the potential to inhibit agricultural food production in its current form. However, they differ in their primary impacts. While loss of industrial civilization is projected to impact the availability of modern technological advances in agriculture, global catastrophes like nuclear war would result in severe climatic changes, rendering most of the earth's surface too cold for agriculture. Still, loss of industrial civilization and societal collapse are likely to ensue in the aftermath of a nuclear war as a secondary impact and add another dimension of catastrophic consequences.

Society is highly dependent on modern agriculture as it enables most of the population to occupy themselves with tasks beyond food production (Coates, 2009; Sandberg, 2018; Smil, 2017). This remarkable surplus in food and energy production can only be maintained through high external inputs into the production system in the shape of machinery, fertilizers, and pesticides (Alston & Pardey, 2014; Miedaner, 2005; Smil, 2017). Certainly, it applies to countries in differing severity as there is no one uniform agricultural production system and stark differences between countries and world regions remain. However, following Manheim (2020) the global food production system can be identified as a fragile system which is prone to systemic cascading failures (Goldin & Vogel, 2010; Helbing, 2013). Hence, even countries with lower industrial dependence are part of the increasingly connected global system and thus, likely to be subjected to the ripple effects of cascading failures. These properties, high industrial dependence and global interconnectedness, have only developed within the last 100 years (Smil, 2017) but have quickly disseminated and profoundly and lastingly changed society. The Carrington event of 1859 is one of the most extreme, documented magnetic storms (Hayakawa et al., 2019). At the time the damages were limited to outages of telegraphic communication but if an event of this magnitude happened today it is

estimated to cause damage ranging in the trillions of dollars with long-lasting consequences (Schieb & Gibson, 2011)

2.2 Loss of Industrial Civilization Scenarios

As shown above the risk categories differ widely in their consequences for global food production. In this work the expected change in agricultural yield if industrial infrastructure is compromised is examined, therefore, the possible causes for a global disruption to industry are presented more in depth. The premise of all these risks is a global scale disruption of the electrical grid. Due to the global industry's and society's dependence on electricity, a global electrical failure would result in a de facto standstill of most industries and machinery. The probability for a losing industry catastrophe in this century is estimated at about ten percent (Mekhaldi et al., 2015). The three dominant potential failures include:

High Altitude Electromagnetic Pulses (HEMP) are a consequence of nuclear detonations high up in the atmosphere. The altitude needed to generate damage over a large area prevents direct damage to humans but may instantaneously cause damage to most electronics. If a nuclear warhead is detonated the emitted gamma rays interact with the atmosphere and create an intense electromagnetic pulse (EMP) which spreads across large distances at the speed of light. The electromagnetic disruption causes overvoltage in electronics similar to a lightning strike but with a higher intensity (Wilson, 2008). The affected area depends on the power and altitude of the detonation, but Wilson (2008) describes a possible scenario where one detonation could affect the entire continental United States. Therefore, a coordinated attack with multiple warheads or the detonation of multiple warheads during a nuclear conflict could lead to large parts of the world being affected simultaneously, resulting in a global catastrophe of unprecedented proportion in the modern era. Especially critical pieces of infrastructure like Large Power Transformers (LPT) could delay recovery for years. LPT are responsible for transforming high voltage electricity used to send energy over long distances to low voltage electricity required for local distribution and consumption, and vice versa (Office of Electricity Delivery and Energy Reliability [OE], 2014). They are mostly highly customized to specific needs which makes their production time and money intensive: under normal conditions LPTs have lead times of 12-24 months (North American Electric Reliability Corporation [NERC] & U.S. Department of Energy [DOE], 2010) or more and cost between $2 to $7.5 million excluding transportation

and installation (Electrical Engineering Portal [EEP], 2013). Further LPTs are very heavy and the US Department of Energy worries about the ability to replace them under crisis conditions (OE, 2014).

A second, similar risk is posed by *Solar Storms.* Solar activity during storms can present itself in the form of solar flares, coronal mass ejections (CME) or both. Solar flares are outbursts of x- and gamma rays and extreme ultraviolet radiation which can disrupt communication technology (National Science and Technology Council [NSTC], 2019). Weiss and Weiss (2019), however, rate it as a minor risk and rather emphasize the effect of coronal mass ejections on the American power grid. This type of solar activity releases supercharged plasma particles towards earth, creating a geomagnetic storm which acts like a natural EMP towards the electrical grid with potentially devastating consequences (Cooper & Sovacool, 2011; NSTC, 2019; Talib & Mogotlhwane, 2011; Weiss & Weiss, 2019). Like HEMPs, CMEs can permanently damage LPTs and potentially cause power outages lasting for years (NSTC, 2019).

Thirdly, globally coordinated *cyber-attacks* on many electrical grids or critical industrial infrastructure pose a threat on a global catastrophic scale. Recorded electrical failures, which have been attributed to targeted cyber-attacks, include a nine-hour power outage in up to eight regions in Ukraine in 2015 (Zetter, 2016) and the destruction of enrichment centrifuges in Iran in 2009/2010 by Stuxnet (Wikipedia, 2021).

Apart from the specific scenarios described above, the fragile world hypothesis introduced by Manheim (2020) can also induce or aggravate a loss of industry scenario. Manheim (2020) states that the world has become increasingly more complex, interconnected and most importantly less resilient. The economy's incentives to minimize redundancy have led to systems' becoming progressively more fragile and hence more vulnerable to disruptions. According to Manheim (2020) a critical system's fragility can cause global catastrophes even severe enough to result in human extinction. Moreover, fragile systems can significantly worsen the impact of one of the LoI scenarios by leading to faster and more severe systems' collapses during a catastrophe.

2.3 Resilience and agriculture

Multiple scholars have highlighted the importance of being prepared to manage the consequences of GCRs and have called for mitigation and resilience efforts (S. D.

Baum et al., 2015; see e.g. Maher & Baum, 2013; Manheim, 2020; Sandberg, 2018). There have been concerns in the past that having a "back-up plan" could increase the possibility of man-made catastrophes like nuclear war but most agree that it is unlikely and rather argue that planning ahead is imperative because it could save billions of lives (for an in-depth discussion of ethical concerns about preparing for a disaster refer to chapter 9 in Denkenberger & Pearce, 2014).

The current COVID-19 pandemic has illustrated very well what happens if a catastrophe hits unprepared and why resilience of critical systems is important. Prevention is always preferred over mitigation, but COVID demonstrates that prevention is not always possible even if the risk class is known and fairly well understood. Further, it serves as a reminder that a low probability for a risk does not prevent it from occurring at any given time. The consequences of the lockdowns show, moreover, the vulnerability of global and interconnected critical systems but also of society itself to disruption. Even though most countries were able to maintain the supply of essential goods, fear and uncertainty of consumers led to hoarding and panic buying which created artificial shortages and even more panic. The interferences in the economy and the need for COVID protection and containment measures have cost the global community billions of dollars and at the same time, up until now, 4.5 million lives (October 2021). The COVID pandemic makes a compelling case for preparing for catastrophes especially considering that in many regions essential businesses have been kept reasonably stocked and open throughout the heights of the pandemic. Resilience efforts for the food production system vary depending on the type of catastrophe. For sun-blocking scenarios like a supervolcano eruption this includes the exploration and preparation of alternative resilient foods such as leaf concentrate, mushrooms grown on logs, bacteria-digested fibre or bacteria fed on natural gas (for an initial presentation and exploration of possible food sources refer to Denkenberger & Pearce, 2014). Most of these sources, however, depend on industrial infrastructure. Therefore, for LoI scenarios the adaptation of classical agricultural practices is the main component to ensure provision.

In previous work Cole, Denkenberger, Griswold, Abdelkhaliq, and Pearce (2016) explored consequences of LoI scenarios for food security and possible mitigation options. Global agricultural productivity was estimated to revert to preindustrial levels. Strategies for increasing potential available food are presented including the

reduction of food waste in all stages, the recovery of plant nutrients from landfills, buildings and human and animal waste and the relocation of people from cities to the fields and from densely to sparsely populated countries. Further options to feed everyone encompass resilient food sources which do not require industrial infrastructure and the expansion of planted area into forests and non-food land uses. Society is highly dependent on modern agriculture as it enables most of the population to occupy themselves with tasks beyond food production (Coates, 2009; Sandberg, 2018; Smil, 2017). This remarkable surplus in food and energy production can only be maintained through high external inputs into the production system in the shape of machinery, fertilizers, and pesticides (Alston & Pardey, 2014; Miedaner, 2005; Smil, 2017). Certainly, it applies to countries in differing severity as there is no one uniform agricultural production system and stark differences between countries and world regions remain. However, following Manheim (2020) the global food production system can be identified as a fragile system which is prone to systemic cascading failures (Goldin & Vogel, 2010; Helbing, 2013). Hence, even countries with lower industrial dependence are part of the increasingly connected global system and thus, likely to be subjected to the ripple effects of cascading failures. These properties, high industrial dependence and global interconnectedness, have only developed within the last 100 years (Smil, 2017) but have quickly disseminated and profoundly and lastingly changed society. The Carrington event of 1859 is one of the most extreme, documented magnetic storms (Hayakawa et al., 2019). At the time the damages were limited to outages of telegraphic communication but if an event of this magnitude happened today it is estimated to cause damage ranging in the trillions of dollars with long-lasting consequences (Schieb & Gibson, 2011).

3 Methodology

All statistical calculations were conducted in Python 3 (Version 8.10) using Anaconda on a Windows PC. The entire code as well as the output datasets are available on github (https://github.com/allfed/LosingIndustryCropYields). Input datasets are freely available online. Links to the resources are provided in Table 1. Visualizations were created in QGIS (Version 3.16.18).

3.1 Selection of model crops and influencing factors

The *crops* modelled in this thesis were chosen based on their status as staple crops both historically and current. Except for the Incas all ancient civilizations were based on cereals, including maize, rice, and wheat (Miedaner, 2005). All three crops are still very important for peoples' diets today. Wheat is by far the most important food crop, providing 20% of daily calories and proteins worldwide (Shiferaw et al., 2013 based on FAOSTAT data in 2012). Its status is derived from being the clearly dominating cereal in developed countries, counting with almost 75% of the daily calories and 81% of the daily proteins from cereals (Shiferaw et al., 2013). In developing countries rice supplies the most calories (about 45% of daily cereal calories), constituting a staple for more than half the world's population (Seck, Diagne, Mohanty, & Wopereis, 2012). Maize is also an important food staple in most developing countries, but its share is substantially smaller (Branco 2020). This is mainly due to the stark increase in demand for maize as livestock feed which amounts to 63% of global maize production (Shiferaw, Prasanna, Hellin, & Bänziger, 2011). The last crop examined in this analysis is soybean which counts with the fourth largest production area after the other three crops. However, it is far less relevant for food intake as only 2% of the global production is directly used for human consumption (Hartman, West, & Herman, 2011). Like maize, the largest share of global production is used as livestock and aquaculture feed. Therefore, both crops have an enormous potential in a LoI scenario because large shares of production can be diverted to direct human consumption. Apart from the potential use shift, soybean is the only legume and the only oil crop considered in the analysis. Legumes could play a crucial role for nitrogen availability in the soil in absence of industrial fertilizers and soybean is the globally most widely produced legume.

Yield-influencing factors can be divided into growth-defining, growth-limiting, and growth-reducing components (Rabbinge, 1993). Growth-defining factors include

climatic conditions like solar radiation, temperature, and crop characteristics. They can't be changed but rather constitute the environmental boundaries for crop growth. Water and nutrient availability are growth-limiting factors which can be influenced by management decisions. Pests and diseases on the other hand reduce yield and can endanger whole harvests.

Even though growth-defining factors can't be managed and aren't of interest in this analysis, climatic variables are included in the model to control for their influence on crop growth. Nonetheless, the focus rests on the manageable two factor classes. The literature offers an abundance of yield-influencing factors (Branco, 2020; Neumann, Verburg, Stehfest, & Müller, 2010; see e.g. Rabbinge, 1993; M. van Ittersum et al., 2003). The factors for the analysis at hand were chosen based on two selection criteria: first, factors were selected based on the key differences between modern and preindustrial agriculture, then factors with insufficient data availability (spatial data at five arcminutes resolution and global scale) were eliminated. Smil (2017, p. 316), Alston and Pardey (2014) and Evenson and Gollin (2003) identified increased inputs in machinery, fertilizer, water, and pesticides in combination with improved varieties as the main drivers for the steep increase in yields. For all listed factors except for improved varieties data availability allowed the inclusion into the analysis.

3.2 Input data and Pre-Processing

As described above, global spatial datasets were sourced for each factor as well as for yield under current conditions. Datasets were selected at five arcminutes resolution when available. The datasets used in the analysis are compiled in Table 1. In the following the data will be presented briefly. For a detailed description of the methodology refer to the respective papers.

Crop yield data for maize, rice, soybean, and wheat were taken from "SPAM2010" (Spatial Production Allocation Model) datasets presented by Yu et al. (2020). The maps are produced by disaggregating non-spatial crop statistics across farming systems and then allocate these values to a spatial grid using an optimization process based on multiple yield-influencing statistics. In the analysis the yield in kg per hectare per grid cell and the area in hectare per grid cell across all production systems are used.

Table 1: GLM Input datasets

Dataset	Definition	Spatial resolution	Temporal reference	Source	Available online
SPAM	Yield (kg/ha), harvested area (ha/cell)	5 arcmin	2010	Yu et al. (2020)	https://doi.org/10.7910/DVN/ PRFF8V
GAEZ v4 AEZ Factors	Thermal regime class, Moisture regime class, Soil/terrain related classes	5 arcmin 5 arcmin 30 arcsec	2010	Fischer et al. (2021)	https://gaez.fao.org/pages/data-viewer
PEST-CHEMGRIDS	Application rate (kg/ha) of 20 active ingredients for 10 dominant crops and 4 aggregated crop classes	5 arcmin	2015	F. Maggi, Tang, La Cecilia, and McBratney (2020)	https://doi.org/10.7927/weq9-pv30
Global Map of Irrigation Areas - Version 5	Area equipped for irrigation (% of total area)	5 arcmin	2005	Siebert, Henrich, Frenken, and Burke (2013)	https://data.apps.fao.org/map/catalog/srv/api/records/f79213a0-88fd-11da-a88f-000d939bc5d8
Gridded nitrogen and phosphorus fertilizer use	N and P application rate (g/m²)	0.5◦degree	1900-2013	Lu and Tian (2016)	https://doi.pangaea.de/10.1594/PANGAEA.863323
Global gridded dataset of manure nitrogen production and application	N manure application (kg/km²)	5 arcmin	1860-2014	Zhang et al. (2017b)	https://doi.pangaea.de/10.1594/PANGAEA.871980
A global gridded data set on tillage (V. 1.1)	Six tillage systems (dominant system/cell)	5 arcmin	Around 2005	Porwollik, Rolinski, and Müller (2019)	https://doi.org/10.5880/PIK.2019.009

As discussed above, only high-level *climatic variables* are included as the goal of the prediction is to assess the lack of anthropogenic inputs without climatic changes. The Agroecological Zones (AEZ) classification is a part of the global AEZ methodology (version 4) and is introduced as a framework for broad-scale analysis and planning (Fischer et al., 2021). The AEZ classes are defined by a combination of temperature regime, moisture regime and soil/terrain related classes. The soil/terrain related classes include an irrigation class which renders redundant information as the actually irrigated area per cell was incorporated into the analysis as a separate variable (see below). Therefore, instead of the combined AEZ classes, the temperature regime, the moisture regime, and the soil/terrain related classes are

included as separate variables. This ensures that only the soil/terrain related classes contain some redundant information within the irrigation category and limits the number of total categories. While thermal and moisture class datasets are available at five arcmin resolution, the soil/terrain dataset is provided at 30 arcsec resolution. To fit the target resolution, it was downsampled to five arcmin. Table 2 gives an overview over the individual classes of the thermal regime, the moisture regime and the soil/terrain related conditions.

Table 2: List of AEZ temperature regime, moisture regime and soil/terrain related classes (Fischer et al., 2021).

Temperature Regime Classes	Moisture regime classes	Soil/terrain related classes
TRC1=Tropics, lowland	M1=LGP < 60days	S1=Dominantly very steep terrain
TRC2=Tropics, highland	M2=LGP 60-120 days	S2=Dominantly hydromorphic soils
TRC3=Subtropics, warm	M3=LGP 120-180 days	S3=No or few soil/terrain limitations
TRC4=Subtropics, moderately cool	M4= LGP 180-225 days	S4= Moderate soil/terrain limitations
TRC5=Subtropics, cool	M5= LGP 225-270 days	S5=Severe soil/terrain limitations
TRC6=Temperate, moderates	M6= LGP 270-365 days	L1=Water
TRC7=Temperate, cool	M7= LGP 365+ days.	L2=Built-up/Artificial
TRC8=Boreal/Cold, no permafrost		L3=Irrigated soils.
TRC9=Boreal/Cold, with permafrost		
TRC10=Arctic/Very cold.		

For *irrigation* the fraction of actually irrigated cropland per cell was calculated based on the "Global Map of Irrigation Areas - Version 5" (Siebert et al., 2013) by multiplying the area equipped for irrigation in hectare per cell with the area actually irrigated as percentage of the area equipped for irrigation per cell. The irrigated areas were determined using subnational statistics derived from national census data or irrigation sector studies. The subnational unit values were then allocated to grid cells by aligning regional and local irrigation maps from various sources with satellite imagery on irrigation areas or other related factors if irrigation data was missing (Siebert et al., 2013). They report that layers for areas equipped for irrigation are much more reliable than layers on actually irrigated areas and water sources because the alignment process was only applied to the layers containing areas equipped for irrigation.

The "PEST-CHEMGRID" dataset provides spatially explicit layers of the application rates of 20 most used active ingredients in kg per hectare per cell for six dominant crops and four aggregated crop classes (F. Maggi et al., 2020). It is based on the USGS Pesticide National Synthesis Project (USGS/PNSP) which compiled the application mass of all active ingredients for 48 US States. Emanating from this

dataset application rates for the 20 most important pesticides were calculated for the US in the base year of 2015. Together with 20 globally gridded environmental quantities the US rates were used in a polynomial extrapolation to estimate values for the rest of the world. Afterwards the data was corrected for local pesticide restrictions (EU) and the usage of GM crops and harmonized against the FAOSTAT country-level values. For the analysis a *pesticide variable* for each crop was compiled by summing up the active ingredients in each cell. The upper bounds of the range for each active ingredient were chosen to remain conservative for the catastrophe yield predictions. Federico Maggi, Tang, La Cecilia, and McBratney (2019) state that the selected ingredients account for 84.2% of pesticide usage in the US in 2015.

Nitrogen (N) and phosphorus (P) fertilizer application rates were taken from the most recent available year of the "Half-degree gridded nitrogen and phosphorus fertilizer use for global agriculture production during 1900-2013" dataset compiled by Lu and Tian (2016). They used total country application mass provided by the International Fertilizer Association (IFA) and the Food and Agriculture Organisation (FAO) and harvested area per grid cell derived from the M3-crop data to calculate tabulated application rates. The tabulated was then interpolated to achieve a half-degree gridded distribution and subsequently harmonized with IFA totals (Lu & Tian, 2017). As the half degree resolution does not align with the other datasets, the layers were upsampled to five arcmin resolution. The unit of the application rates are given as g per m² which was converted to kg per hectare to match the unit of the crop yield.

The "Global gridded dataset of manure nitrogen production and application" (Zhang et al., 2017b) supplies spatially explicit *manure production and application rates* in kg per km² per cell at five arcmin resolution. The manure production rate was calculated using the distribution of livestock provided by the Global Livestock Impact Mapping System (GLIMS), the animal-specific excretion rates from the Intergovernmental Panel on Climate Change (IPCC) 2006 guidelines and FAOSTAT data to trace yearly changes in livestock populations. The manure application rate was estimated based on the spatial distribution of different livestock management systems in different agroecological zones (Zhang et al., 2017a). As for the fertilizer application rate, the values were converted to kg per hectare to match the crop yield unit. The most recent available year was used for the analysis.

The N manure and N fertilizer application rate datasets presented above were summed up into a combined N total layer. This was done because the interest of the analysis lies with the effect reduced N input has on yield and not with the effect of N input from different sources. Moreover, it was taken as a measure to reduce the number of variables and possible multicollinearity between them.

Mechanization is the only selected factor which required the use of a proxy as no spatially explicit data on the degree of mechanisation in agriculture was available. The "global gridded data set on tillage (V. 1.1.)" created by Porwollik, Rolinski, and Müller (2019) served as surrogate. Tillage practices were classified into six tillage systems according to literature findings, namely:

- 1 = conventional annual tillage
- 2 = traditional annual tillage
- 3 = reduced tillage
- 4 = Conservation Agriculture
- 5 = rotational tillage
- 6 = traditional rotational tillage.

The tillage systems were allocated to gridded cropland areas at five arcmin resolution based on spatial datasets for crop type, water management regime, field size, water erosion, income, and aridity (Porwollik, Rolinski, Heinke, & Müller, 2019). A large factor for the classification of tillage systems is the involvement of heavy machinery as it facilitates mixing soil in greater depth. Hence, it is possible to determine which systems rely on machinery for tilling and which do not by means of the decision tree and the characteristics of the tillage systems presented by Porwollik, Rolinski, Heinke, and Müller (2019). It is reasonable to assume other farm activities such as sowing, and harvesting are also carried out with machinery if tilling is mechanized. Therefore, the tillage systems are reclassified into either 0 = non-mechanized or 1 = mechanized: tillage systems 2, 3 and 6 are classified as 0 and systems 1, 4 and 5 as 1. Conservation agriculture is classified as mechanized even though tillage is reduced to almost zero because currently conservation agriculture is most widely adopted in North and South America and Australia (Kassam, Friedrich, & Derpsch, 2019) where agriculture tends to be mostly mechanized. The dataset provides separate layers for 42 different crop types but in the analysis a combined layer is used so that a larger area is covered. It is assumed

that regions with highly mechanized cropping systems for one crop generally do not farm other crops by hand or with animals.

3.3 Statistical yield modelling

Before the linear model can be fitted, the input data must be cleaned and pre-processed to allow for a sensible analysis. For processing the individual datasets described above are imported into Python and compiled into one data frame. This allows rows to be eliminated on the condition of one column. The following operations were carried out for each crop individually.

The values for crop yield in kg per hectare in each cell represent a varying portion of the specific crop's harvested area ranging from 0.1 to 19,344.3 ha. This is a very large range which can influence the results of the analysis. Therefore, all rows containing values for harvested area below 100 ha were dropped from the data frame. This operation led to the deletion of 44-72% of all data points. However, these cells contributed only between 1.6-3.2% of the total global crop yield summed up over total crop specific harvested area.

After dropping the cells with an area below 100 ha missing values in the remaining datasets were addressed. The pesticides and mechanisation data still contained many missing values. As there is no established linear dependence of pesticides and mechanisation on the other variables it is refrained from a linear imputation. Due to a high number of available data points the rows containing missing values for pesticides and mechanisation are dropped.

In the N and P fertilizer columns missing values only amounted to 1-2.3% of total data points. Following the previous operations between 80% and 94% of the missing data rows were already dropped. Therefore, it was decided to fill the remaining cells with the forward filling method: the missing data point was substituted for the value of the preceding cell.

The temperature and moisture regime columns had very few missing data points and as the different classes in the regimes each cover largely homogeneous zones, the affected cells were filled with the forward filling method as described above. The soil/terrain related column contained more missing values and cells classified as built-up/artificial (L2) or as water bodies (L1). These classes are unexpected in a data frame containing only cells where crops are grown on large parts of the cell area. This discrepancy is probably due to the downsampling process as the result wasn't harmonized against a cropland dataset. Considering that the number of

missing and misclassified values ranged around the same percentage (1.6-2.2%) as the N and P fertilizer missing values and was also substantially diminished by previous operations the forward filling method was applied.

The descriptive statistics and boxplots of the individual variables exposed the presence of implausible values in the N and P fertilizer, the manure, and the yield columns. To prevent clear *outliers* from skewing the relationship, all rows with values above the 99.9^{th} percentile for N and P fertilizer, manure, N total and yield were dropped. Given the distribution of the remaining values and the values commonly reported in the literature, these data points are more likely to be errors in the input datasets than real information characterizing the relationship between yield and input factors. The cut-off point was chosen conservatively because the remaining high values for yield and nutrient application rates are unlikely but possible to be observed in a real-world context.

As a first approach to detect multicollinearity, the correlations among the variables (excluding yield) were tested by calculating a correlation matrix based on Spearman's rank correlation coefficient ρ. No correlations indicated possible collinearity except for the correlation between N total and P fertilizer for three out of four crops (maize: $\rho=0.82$, rice: $\rho=0.91$, soybean: $\rho=0.53$, wheat: $\rho=0.87$). This correlation is unsurprising as N fertilizer makes up a large part of N total and N and P fertilizer are usually applied together as compound fertilizer. To further investigate the presence of *multicollinearity*, the variance inflation factor (VIF) was calculated for each continuous variable and for each level of the categorical variables. The VIF confirmed the multicollinearity between N total and P fertilizer and pointed towards strong multicollinearity between the classes of the temperature and the moisture regime. The literature contains different threshold values for when the VIF indicates serious multicollinearity. The most prominent thresholds are specified as everything above 5 constitutes the need for action (Huang, 2014) or as values above 10 give reason for concern (Fox, 2002). The VIF of N total and P fertilizer remain below 10, depending on the crop they range from 6.2-8.6 for N total and from 4.5-8.9 for P fertilizer with the highest values being present in the rice dataset. As the values do not surpass 10 it is decided to keep both variables in the model as P and N availability could vary substantially in the scenario of interest. The VIF values for the temperature and moisture regime classes surpassed both thresholds by far ranking as high as 120 in some instances. Those remarkably high

values can be ascribed to an uneven distribution of observations among the classes. For the temperature regime the differences were particularly stark as the coldest three climate classes counted with very low numbers of observations. To resolve the issue class TRC7-TRC10 were combined into a new TRC7 class encompassing Temperate cool, Boreal and Arctic temperatures. The uneven distribution of observations in the moisture regime was addressed by fusing the two lowest (M1 and M2) and the two highest classes (M6 and M7) into one new class each: M1 = LGP < 120 days and M5 = LGP 270+ days. Some stronger collinearity remained in the rice dataset which could have been addressed by combining more classes in the temperature regime. However, this was not implemented as the distribution of classes varied widely between the different crops and it would have been difficult to find a combination which improved rice while not introducing new collinearity into other datasets. Adding the variables consecutively to the model did not show any abnormalities in the standard errors, p values or the root mean gamma deviance (RMGD).

A split-sample approach is applied to *validate* the model. Prior to fitting the model, 20% of the pre-processed data are randomly selected. This sample is used for validation while the model is *calibrated* on the remaining 80% of the data points.

As the dependent variable cannot assume negative values, the distribution of the data points is strongly right skewed for all crops and the residual are non-normally distributed, the assumptions for a classic multiple regression on a normal distribution are violated. Therefore, a generalized linear model (GLM) based on a gamma distribution is fitted to the data. The link function is assumed to be the natural logarithm. The model is specified as followed:

$$Y \sim Gamma(shape, scale)$$

where:

$$g(shape) = \ln(shape) = \mathrm{f}(X_i; \mathrm{b}) = b_0 + b_1/x_i$$

The model is fitted with a simple linear relationship and no interactions. The categorical variables are coded as dummies. To assess model fit McFadden's ρ^2 is calculated. The RMDG serves as a measure for model transportability. The significance level is set at $\alpha = 5\%$.

3.4 Yield prediction

Crop yields are predicted for a worst case LoI scenario. It is assumed that a catastrophe disables power supply globally and effectively inhibits industrial

production, communication, transportation, and all other services relying on electricity. The electrical outage is expected to be immediate but the effects on agricultural production are likely buffered by stocks in storage. Hence, the period following the catastrophe is divided into two phases: phase 1 comprises the first year after the catastrophe where stocks are still available while phase 2 starts in year 2 after stocks are depleted and the consequences of losing electrical infrastructure take full effect. The datasets of the independent variables used in the calibration of the model are modified for the predictions according to the assumptions for each phase as outlined above.

Phase 1 assumes sufficient stocks in above-ground fossil fuels to fully power agricultural machinery for another year. The International Energy Agency (IEA, 2020) states the annual demand of the agricultural industry in oil products at 111,062 thousand tons of oil equivalent (ktoe) in 2018. Available above-ground fuel in a LoI catastrophe was estimated at 319,000 ktoe, encompassing 172,000 ktoe of gasoline and 147,000 ktoe of diesel, by Cole et al. (2016). Considering that most agricultural machinery runs on diesel, the estimated stocks last for about a year while leaving the gasoline for critical transportation. Thus, the *mechanisation* input dataset remains unchanged for phase 1.

All following calculations for the phase 1 input datasets are carried out under consideration of all cells where harvested area for the respective crop is greater than zero. Even though a large percentage of these cells were not considered for model calibration and are not contributing to the predictions, these areas would still need agricultural inputs in a catastrophic scenario. To account for this, all cells are included in the distribution of available stocks. Only values above the 99.9th percentile of the respective variable are excluded as they do not represent reasonable data points.

N and P fertilizer application rates for phase 1 are calculated based on the annual global surplus for each nutrient reported by the Food and Agriculture Organization of the United Nations (2017). They project a surplus of 14,477 thousand t of nitrogen and 4,142 thousand t of phosphorus in 2020. In a first step the amount of the nutrient applied in each cell is calculated as a fraction of the total amount of the nutrient summed over the crop-specific harvested area with:

$$N_{frac} = \frac{N_{fert} \times A_C}{\sum N_{fert} \times A_C}$$

where N_{fert} is the application rate of the nutrient in kg per ha per cell and A_C is the crop-specific harvested area in ha per cell. Then, the new total amount of the nutrient available for the specific crop in phase 1 is calculated based on the surplus reported by the FAO (2017).

$$N_{TC} = \frac{\sum N_{fert} \times A_C}{T_{NG}} \times T_{NG1}$$

where T_{NG} is the total amount of the nutrient projected to be used for crop fertilisation in 2020 and T_{NG1} is the projected nutrient surplus in 2020. The total amount of nitrogen used for crop fertilization is projected to be 118,763 thousand t and the amount of phosphorus is estimated at 45,858 thousand t in 2020 (FAO, 2017). Lastly the new total is allocated back to the cells based on N_{frac}:

$$N_{fert1} = \frac{N_{TC} \times N_{frac}}{A_C}$$

The *pesticide application rates* for phase 1 are calculated with the same approach as the fertilizer application rates. However, no data was available on the surplus of pesticides generated in one year. Therefore, it was assumed that the surplus' share of global pesticide production was in the same range as the share of the nutrients' surplus in the global nutrient production. Equation 2 and 4 remain unchanged but the new total of pesticides available for a specific crop in phase 1 is calculated as follows:

$$P_{TC} = \frac{\sum P_H \times A_C}{T_{PG}} \times T_{PG} \times \frac{\frac{T_{nG1}}{T_{nG}} + \frac{T_{pG1}}{T_{pG}}}{2}$$

where P_H is the pesticide application rate in kg per hectare per cell, T_{PG} is the total amount of pesticides used for agricultural purposes in 2019 (FAOSTAT, 2021b) and T_{nG1}, T_{nG}, T_{pG1} and T_{pG} referring to the totals defined above for nitrogen and phosphorus respectively.

In phase 2 all stocks are assumed to be depleted, hence, mechanisation2, n_{fert2}, p_{fert2} and P_{H2} are set to zero.

Manure application rates are expected to be the same for phase 1 and 2 as they are dependent on the available livestock. It is assumed that the population would switch to a mostly vegan diet to use the calories which can be produced in the most efficient way possible. Therefore, only draft animals like horses, buffaloes and cows will be kept and fed on agricultural residues and roughage. For this analysis only cows will be considered as the calculations are based on the numbers provided by Zhang et

al. (2017a) who didn't include horses and buffaloes as they currently constitute only a very small percentage of the global livestock population and are even less important for manure production and application in modern agricultural systems. To calculate new manure application rates, the labour demand in each grid cell is assessed in terms of needed cows per grid cell by dividing the harvested area in each cell by the area which can be worked by one cow (ha per cow). Prak (2006) reported 7.4 hectare per draft animal as a typical working capacity. Considering that modern cattle are not bred to work this value can be expected to be considerably lower. To be conservative in terms of manure availability 5 hectare per cow were used for the calculations. The next step was to calculate the excretion rate of one cow. Zhang et al. (2017a) provided the total amount of manure produced in 2014 which amounts to 131,000 thousand t of N and the share of the manure produced by cattle, namely 43.7%. (FAOSTAT, 2021a) reported 1.44 billion heads of cattle in 2014. Multiplying the total amount of manure with the fraction attributed to cattle and dividing the result by the heads of cattle in that year rendered an excretion rate of ~ 40 kg per cow per year. In the last step the new crop specific N manure application rate was computed by:

$$M_{nC} = \frac{39.77 \times C_C}{A_C}$$

where C_C is the crop specific number of cows in each grid cell.

For phase 1 M_{nC} was combined with n_{fert1} into n_{tot1}. In phase 2 the N from manure is the only source of N left so it is taken as the sole input.

As with manure, *irrigation* as a fraction of the cropland in a cell which is actually irrigated is not affected by first year stocks and therefore the same values are used for phase 1 and phase 2. A sharp reduction in actually irrigated area is expected as large part of the irrigation infrastructure are dependent on electricity. To obtain the fraction of irrigated area, which is reliant on electricity, Rivers (2021) combined the information on the source of the irrigation water (surface or groundwater or other) with country-level statistics. For an in-depth description of the methodology refer to Rivers (2021). The fraction of actually irrigated cropland in a LoI scenario was calculated as follows:

$$I_{LoI} = I_{AC} \times (1 - I_{RC})$$

where I_{AC} is the currently irrigated fraction of cropland in each cell and I_{RC} is the fraction of currently irrigated area which is reliant on electricity in each cell.

The datasets comprising the input variables for phases 1 and 2 are fed into the model specified above to predict the crop-specific yields under LoI conditions. The predicted values are used to calculate the crop-specific yield change rate for each cell:

$$YC_{PC} = \frac{(Y_{PC} - Y_C)}{Y_C}$$

where Y_{PC} is the crop-specific predicted yield in the respective phase and Y_C is the crop-specific yield around 2010 taken from the SPAM2010 dataset. Values above zero were set to zero as substantial yield increase in an LoI scenario is very unlikely. Rather, the positive values are taken as an indication for stable yields unaffected by catastrophic circumstances. For the predicted yield and change rate values in each phase descriptive statistics measures were computed, namely the range and the weighted mean. The yield was weighted according to the corresponding harvested area while the change rate was weighted according to the yield in 2010. The mean for the change rates was determined in two different ways. First the mean is based on the predicted values while the second approach took the dataset with the substituted zeros as the computing basis.

Additionally, the overall reduction in yield and in total crop production in comparison to the 2010 value was calculated.

The prediction results were saved as five arcmin ASCII files and visualized in QGIS (Version 3.16.18). To provide a broader overview of large trends, the results were moreover downsampled to a two-degree resolution.

4 Results

4.1 Fitted Gamma GLM

The generalized linear model was fitted for all crops based on the gamma distribution and on the same set of variables which were carefully selected based on the literature. The final model for each crop includes the explanatory variables presented in Table 3. The first class of temperature regime, moisture regime and the soil/terrain related conditions are not listed, as the categorical variables were coded as dummies to be included into the mode. Therefore, the classes TRC1=Tropics, lowland, M1=LGP<120 days and S1=Dominantly very steep terrain are implicit in the intercept. In other words, if all other classes of a categorical variable are coded as zero, it represents a hypothetical 1 for the dropped class. As a result, the intercept is the expected value for crop yield without any external nutrient, water or pesticides inputs, without the use of machinery in a tropical lowland climate with a growing period length below 120 days and in dominantly very steep terrain. The values for the intercepts are similar for all four crops ranging from 605 to 751. Considering that most coefficients have positive impacts on the expected yield, the model cannot capture low yield values very well. All coefficients except for one were significant with α=5%. Only in the model for wheat TRC2 was not significantly different from TRC1. This is probably due to a low number of observations in class TRC2 for wheat. The two classes could have been combined into one but were kept separate to ensure consistency with the models for maize, rice, and soybean.

As described in chapter 3 the models were calibrated with 80% of the data points while the remaining 20% were used for validation. Table 3 contains the values for McFadden's ρ^2 and the Root Mean Gamma Deviance (RMGD) for each crop calculated with (1) the calibration and (2) the validation data points. The validation data calculations supported the estimates based on the calibration data points. The validated ρ^2-value varied strongly across the different crops: the highest agreement between data and model was found for maize with a ρ^2 of 0.47. The GLM for rice had a ρ^2 of 0.41, for the wheat model it was 0.37 and the lowest value was calculated for soybean with 0.34. Still, all values suggest that the models fit the data well. According to McFadden (1977, p. 35), "…, values of .2 to .4 for ρ^2 represent an excellent fit". The RMGD was calculated as a measure of model transportability. The lowest error was computed for soybean with 0.39, followed by rice with 0.49, then wheat with 0.52 and the highest error was found for the maize GLM with 0.59.

Table 3: GLM coefficients of all variables with 95% confidence interval on link and response scale and corresponding p-value for each crop. McFadden's ρ^2 as measure for goodness of fit and Root Mean Gamma Variance as measure for model transportability calculated on the calibration and the validation data points. Variables:TRC2=Tropics, highlands; TRC3=Subtropics, warm; TRC4=Subtropics, mod. cool; TRC5=Subtropics, cool; TRC6=Temperate, moderate; TRC7=Temperate, cool – Arctic; M2=LGP 120-180 days; M3=LGP 180-225 days; M4=LGP 225-270 days; M5=LGP 270+ days; S2=hydro soils; S3=few limitations; S4=mod. limitations; S5=severe limitations; L3=irrigated soils; TRC1, M1 and S1 are implicit in the intercept.

	Maize (n=195,361)			Rice (n_{tot}=93,993)			Soybean (n=77,796)			Wheat (n=210,284)		
	Calibration (n_{cal}=156,289)	Validation (n_{val}=39,072)		Calibration (n_{cal}=75,194)	Validation (n_{val}=18,779)		Calibration (n_{cal}=62,237)	Validation (n_{val}=15,559)		Calibration (n_{cal}=168,227)	Validation (n_{val}=42,257)	
McFadden's ρ^2	0.4794	0.4672		0.41	0.4114		0.3449	0.3431		0.3778	0.3707	
Root Mean Gamma Deviance	0.5828	0.5897		0.4954	0.4913		0.3828	0.3863		0.5194	0.5228	
	Coefficients (link scale) ± 95% confidence interval	Odds ratios (response scale)	p-value	Coefficients (link scale) ± 95% confidence interval	Odds ratios (response scale)	p-value	Coefficients (link scale) ± 95% confidence interval	Odds ratios (response scale)	p-value	Coefficients (link scale) ± 95% confidence interval	Odds ratios (response scale)	p-value
Intercept	6.622 ± 0.023	751.34	0.000	7.385 ± 0.025	1611.61	0.000	6.404 ± 0.043	604.49	0.000	6.501 ± 0.025	665.80	0.000
TRC2	0.145 ± 0.013	1.16	0.000	0.290 ± 0.027	1.33	0.000	0.158 ± 0.022	1.17	0.000	-0.010 ± 0.023	0.99	0.417
TRC3	0.094 ± 0.012	1.10	0.000	-0.135 ± 0.011	0.87	0.000	-0.040 ± 0.013	0.96	0.000	0.221 ± 0.017	1.25	0.000
TRC4	0.55 ± 0.012	1.73	0.000	0.294 ± 0.014	1.34	0.000	0.069 ± 0.013	1.07	0.000	-0.106 ± 0.017	0.90	0.000
TRC5	0.674 ± 0.015	1.96	0.000	0.261 ± 0.022	1.29	0.000	0.140 ± 0.021	1.15	0.000	-0.126 ± 0.018	0.88	0.000
TRC6	0.696 ± 0.011	2.01	0.000	0.348 ± 0.016	1.41	0.000	0.238 ± 0.012	1.26	0.000	0.175 ± 0.017	1.19	0.000
TRC7	0.745 ± 0.011	2.11	0.000	0.343 ± 0.025	1.4	0.000	0.075 ± 0.014	1.08	0.000	0.063 ± 0.017	1.06	0.000
M2	-0.099 ± 0.013	0.91	0.000	-0.082 ± 0.016	0.92	0.000	0.225 ± 0.023	1.25	0.000	0.026 ± 0.008	1.03	0.000
M3	0.060 ± 0.013	1.06	0.000	-0.046 ± 0.017	0.95	0.000	0.297 ± 0.023	1.35	0.000	0.286 ± 0.008	1.33	0.000
M4	0.272 ± 0.013	1.31	0.000	-0.039 ± 0.018	0.96	0.000	0.453 ± 0.023	1.57	0.000	0.459 ± 0.010	1.58	0.000
M5	0.256 ± 0.014	1.29	0.000	0.108 ± 0.016	1.11	0.000	0.451 ± 0.024	1.57	0.000	0.548 ± 0.010	1.73	0.000
S2	0.924 ± 0.027	2.52	0.000	0.503 ± 0.029	1.65	0.000	0.490 ± 0.039	1.63	0.000	0.629 ± 0.023	1.88	0.000
S3	0.909 ± 0.020	2.48	0.000	0.479 ± 0.022	1.61	0.000	0.562 ± 0.036	1.75	0.000	0.645 ± 0.019	1.91	0.000
S4	0.651 ± 0.019	1.92	0.000	0.346 ± 0.020	1.41	0.000	0.401 ± 0.035	1.49	0.000	0.496 ± 0.019	1.64	0.000
S5	0.389 ± 0.022	1.48	0.000	0.057 ± 0.022	1.05	0.000	0.164 ± 0.037	1.17	0.000	0.281 ± 0.022	1.33	0.000
L3	0.956 ± 0.022	2.60	0.000	0.433 ± 0.021	1.54	0.000	0.520 ± 0.037	1.68	0.000	0.734 ± 0.020	2.08	0.000
n_total	-0.001 ± 0.0001	1.00	0.000	0.001 ± 0.0001	1	0.000	-0.002 ± 0.0003	0.99	0.000	0.003 ± 0.0002	1.00	0.000
p_fertilizer	0.011 ± 0.001	1.01	0.000	0.005 ± 0.001	1	0.000	0.013 ± 0.0001	1.01	0.000	-0.014± 0.0008	0.99	0.000
pesticides_H	0.002 ± 0.002	1.00	0.016	-0.014 ± 0.002	0.98	0.000	-0.027 ± 0.003	0.97	0.000	0.386 ± 0.013	1.47	0.000
irrigation_tot	0.477 ± 0.015	1.61	0.000	0.470 ± 0.013	1.59	0.000	0.199 ± 0.017	1.22	0.000	0.290 ± 0.008	1.34	0.000
mechanized	0.386 ± 0.007	1.47	0.000	0.149 ± 0.009	1.16	0.000	0.375 ± 0.012	1.46	0.000	0.279 ± 0.009	1.32	0.000

4.2 Mean predicted yield and crop production changes in a LoI scenario

Descriptive statistics of the predicted yield for each crop in comparison to SPAM2010 crop yields are presented in Table 4. The calculations for the SPAM2010 statistics are based on the cells of the dataset which were used in the analysis excluding all cells as described in chapter 3. Mean yields were computed by weighting each value according to the harvested area in that cell.

In a LoI scenario predicted yields vary substantially between phase 1 and 2 and between crops. For phase 1 yields are predicted to reduce between 10-28%, with soybean counting with the lowest expected reduction of 10% and wheat and rice yields both shrinking by 28%. Phase 2, namely the loss of any industrially produced inputs to agriculture, affected crop yields to a varying extent. While soybean yields were least diminished in phase 1, in phase 2 they dropped by 36% in comparison to SPAM2010 yields.

Table 4: Descriptive statistics of the prediction results for phase 1 and 2 and for the respective SPAM2010 yield data for each crop. SPAM2010 characteristics are based solely on data points used in the prediction analysis.

	Maize (n=195,361)	Rice (n=93,993)	Soybean (n=77,796)	Wheat (n=210,284)
Area weighted mean SPAM2010 in kg/ha	5521	4394	2507	3091
Area weighted mean Phase 1 in kg/ha (positive rates set to zero)	4412 (3920)	3149 (2944)	2257 (2081)	2232 (2032)
Area weighted mean Phase 2 in kg/ha (positive rates set to zero)	3300 (3037)	2955 (2726)	1601 (1534)	1773 (1641)
Total Production SPAM2010 (million t)	762.5	622.4	223.8	597.3
Total Production Phase 1 in million t (positive rates set to zero)	609.4 (541)	446.2 (415.5)	201.5 (186.1)	431.4 (388.4)
Total Production Phase 2 in million t (positive rates set to zero)	455.9 (416.3)	418.8 (393.5)	142.9 (138.3)	342.6 (322.3)
Projected reduction Phase 1 (%)	20	28	10	28
Projected reduction Phase 2 (%)	40	33	36	43
Projected reduction Phase 1 (positive rates set to zero) (%)	29	33	17	35
Projected reduction Phase 2 (positive rates set to zero) (%)	45	37	38	46
Yield range SPAM2010 (kg/ha)	27 - 18,744	111 - 16,053	55 - 5,882	74 – 12,899
Yield range GLM fitted values (kg/ha)	680 - 16,940	1,388 - 12,166	709 - 4,430	611 - 12,849
Yield range Phase 1 in kg/ha (positive rates set to zero)	675 - 12,745 (27 – 11,838)	1,360 - 7,765 (111 – 7,506)	675 – 3,509 (55 - 3,251)	606 - 5,525 (74 – 5,122)
Yield range Phase 2 in kg/ha (positive rates set to zero)	675 - 8,640 (27 – 8,231)	1,355 - 6,587 (111 - 6,320)	675 – 2,443 (55 – 2,443)	602 – 4,311 (74 - 4,311)

This equates to an increased reduction of 26% of the SPAM2010 yields. Rice yields were projected to decrease by 33% in phase 2 but unlike soybean yields, rice yields were already greatly lowered in phase 1. Wheat yields are estimated to face the greatest overall reduction of 43% of the SPAM2010 yields. The predicted yield loss for maize doubled from 20% in phase 1 to 40% in phase 2 compared to SPAM2010 yields. Overall, a full LoI scenario in phase 2 was projected to generate a yield loss of at least one third of the yield prior to the catastrophe (Table 4).

The values described above represent the model predictions including positive and negative changes in individual cells. It is likely, however, that most of the positive change rates estimated by the models are attributable to the GLMs not capturing the lowest SPAM2010 yield values. Therefore, the effect of the positive change rates on the overall yield loss is tested by calculating the mean change rate for each crop in phase 1 and 2 with the positive change rates set to zero. This leads to higher yield losses, but the effect varies across crops and is substantially stronger in phase 1. In phase 1 almost double the number of cells count with positive change rates in comparison to phase 2. The additional reductions range from 5% for rice up to 9% for maize yields. Yields decreased by an additional 2-5% in phase 2, leading to the largest overall reduction increasing to 46% for wheat yields. Discounting positive changes from the projections results in rice and wheat yields already dropping by one third in phase 1 and the projected losses for maize and wheat yields in phase 2 almost amounting to half of the SPAM2010 crop yields. Maize yield predictions were affected most by the changed approach.

To further investigate the properties of the GLMs in comparison to the SPAM2010 dataset and across the two phases with differing severity, the value ranges of SPAM2010 yields and the GLM estimates for current, phase 1 and phase 2 conditions were computed for each crop (Table 4). Table 4 shows that the GLMs in all instances predict a minimum value at least eight times higher than in the original dataset. Only if the positive change rates are set to zero, the minimum value aligns with the minimum of the SPAM2010 crop yields. This confirms the assumption that the models do not fit the small data points very well. Among the model estimates for different conditions minimum values barely differ within one crop which suggests that lower yields are only marginally negatively affected by the LoI consequences. Minimum values were also similar between maize, soybean, and wheat. Rice counted with by far the highest minimum value while the mean of rice

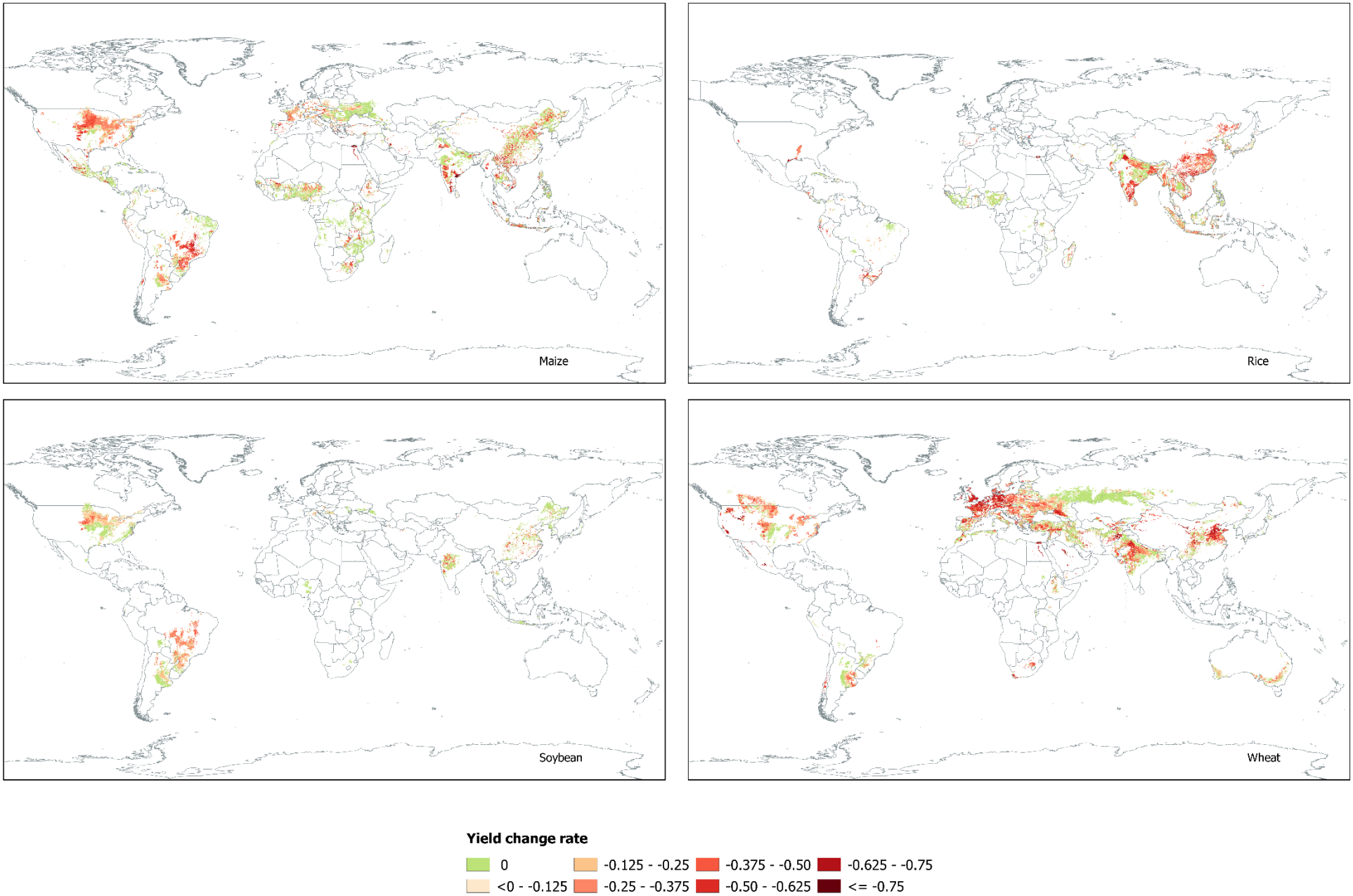

Figure 2: Yield change rate in Phase 1 for each crop at 5 arcmin resolution. Positive change rates are set to zero.

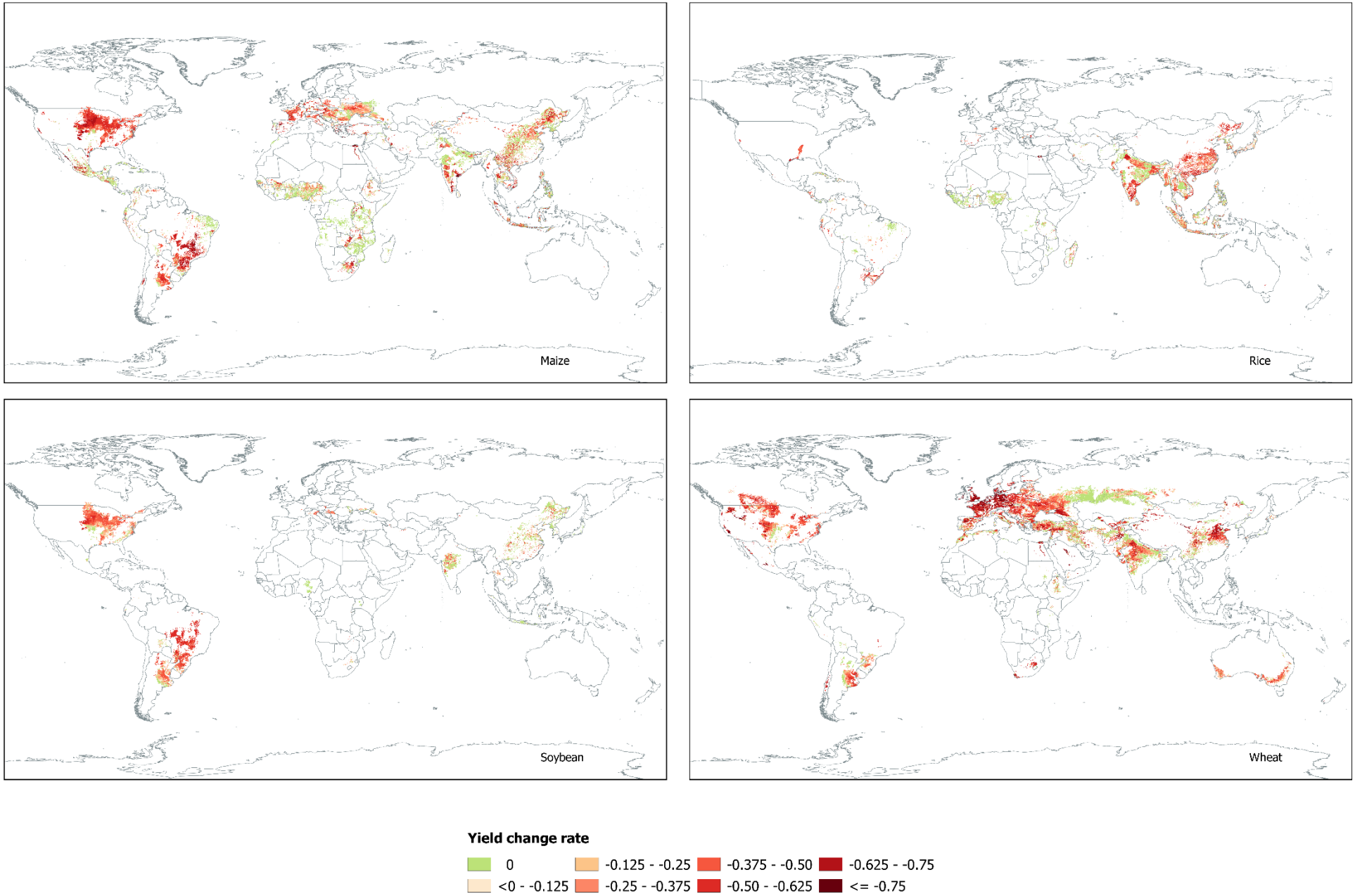

Figure 3: Yield change rate in Phase 2 for each crop at 5 arcmin resolution. Positive change rates are set to zero.

yield ranges lower than maize yield men. The maximum values, on the other hand, were estimated to reduce substantially - as expected - under worsening LoI conditions. However, modelling current conditions with the GLMs also resulted in a considerably lower maximum value, even though the largest values of the SPAM2010 data were dropped before calculating the statistics. The generalized linear models estimate a more moderate range of values than the range found in the SPAM2010 data.

4.3 Gridded predicted yield change rates in a LoI scenario

All gridded yield change results are presented with the positive change rates set to zero for clarity. Figure 2 and Figure 3 show the global spatial distribution of yield change rates for each crop at 5 arcmin resolution in phase 1 (Figure 2) and phase 2 (Figure 3). The gridded presentation allows to identify hotspots which are projected to be strongly affected in a LoI scenario. Figure 3 is used for the hotspot identification as phase 2 represents the full impact of losing industrial inputs and Figure 2 shows that the same regions are affected in phase 1 with less overall severity. The GLM predicted a severe reduction of maize yields in North and South America, Europe, South Africa, Sambia, the Nile region and Southern India. China, Indonesia, and the remaining parts of India showed a highly heterogenous landscape, alternating between strongly and barely affected regions. The same heterogeneity can be found in India and China for soybean yields, in Indonesia for rice yields and in Central China, the Southwestern Caspian region and Ethiopia for wheat yields. Yield loss hotspots for rice were projected to be in China, India, Southern Brazil, the Mississippi region, and the European rice-growing regions. Soybean yields were estimated to be diminished most in North and South America and Central Europe. For wheat highest yield decrease was predicted to occur in Europe, North America, South Africa, Northern Argentina, Northern India, Northeastern China, Southern Australia, and the Nile Region. Over all crops yield loss hotspots largely aligned and differed mostly due to differing distribution of growing area. Globally the areas with the largest negative impacts on yields were projected to be North and South America, Europe, China, India, and Indonesia. Additionally, both figures show that the hotspot regions have higher projected yield losses than the mean predicted reduction presented above. In Phase 1 most critical regions denoted yield reductions above 25% and a large part above 37.5%. In Phase 2 for most hotspots yields were reduced more than half and in the most

severely affected regions, namely South America for maize and rice and Central Europe for wheat yields declined by more than 62.5%.

Figure 5 and Figure 4 show the same data as Figure 2 and Figure 3 but in 2-degree resolution. To create these maps, the GLM results were averaged over 2-degree grid cells. In an analysis testing different resolutions, it was found that averaging the estimated values over 2-degree grid cells yields a better agreement between the SPAM2010 crop yields and the model predictions (McFadden's ρ^2 between 0.35 (soybean) and 0.52 (maize)). By applying this approach model quirks are averaged out to some degree, giving a clearer overview over trends. Moreover, the approach de facto extrapolates the results to a larger area. The extrapolation was not validated but given the largely homogenous distribution of both the strongly and the barely affected regions it seems to be a reasonable assumption.

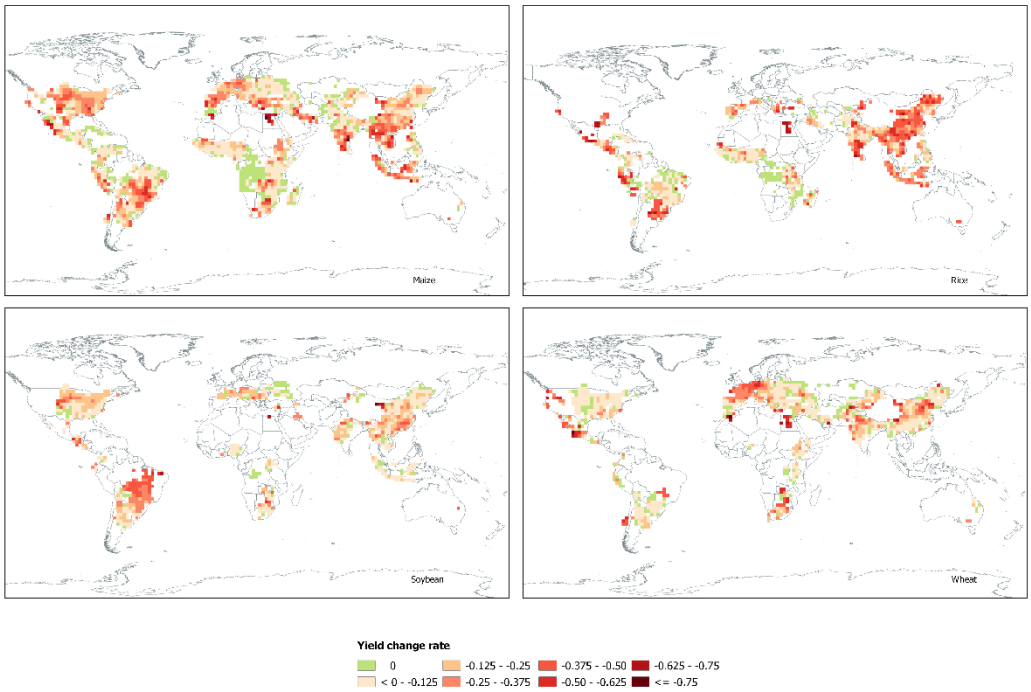

Figure 5: Yield change rate in Phase 1 for each crop at 2-degree resolution. Positive change rates are set to zero.

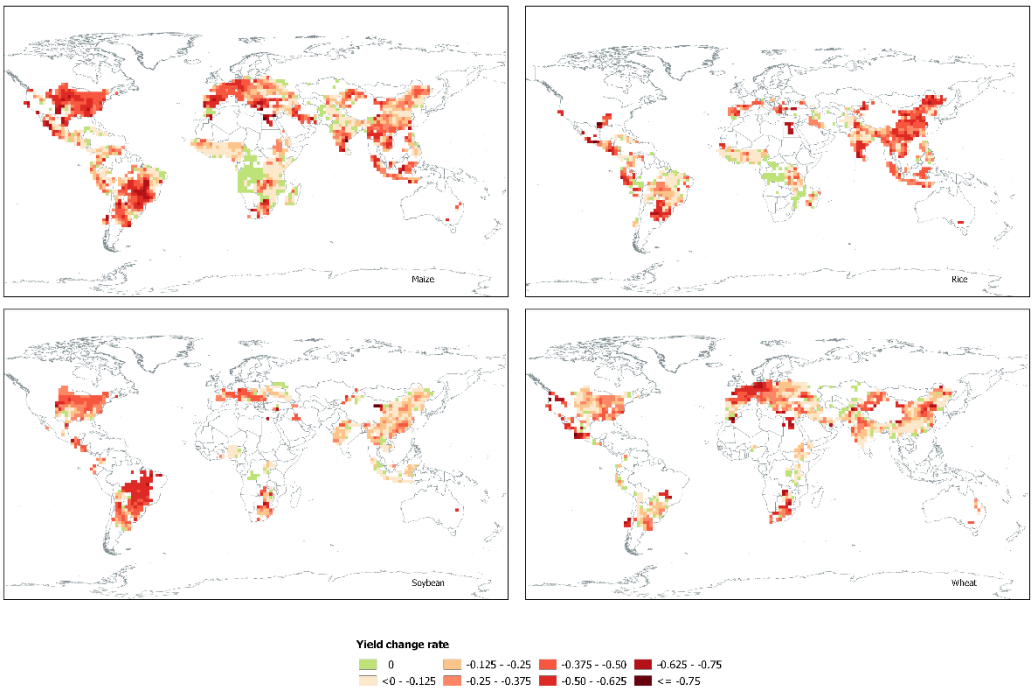

Figure 4: Yield change rate in Phase 2 for each crop at 2-degree resolution. Positive change rates are set to zero.

5 Discussion

Following the first evaluations of the possible effects of a LoI scenario on agriculture by Cole et al. (2016) this work proposes a formal modelling approach to investigate the issue, adds a spatial component to the analysis and examines LoI consequences on agriculture in two different phases. Cole et al. (2016) assume preindustrial agricultural productivity in a LoI scenario which corresponds to a 60% drop from current yield levels. The results at hand suggest that overall yields would only drop between 33% and 46%. Nevertheless, while Cole et al. (2016) describe their estimate as conservative, the results presented above can be considered optimistic. Moreover, individual regions are projected to suffer much larger cuts in productivity firmly surpassing 50% in most cases and ranging up to 90%. Therefore, the predictions should be understood as a first crop-specific and spatially explicit estimate on how strongly yields could be affected by a catastrophic scenario which inhibits global industry and trade. The general trends visible in the prediction results are reliable and can be used as a guideline going forward. However, it is not recommended to use the generated datasets in regional analysis or for detailed response planning. Achieving the necessary level of model accuracy for these applications was beyond the scope of this thesis. In the following the suitability of the modelling approach for the prediction of yields in catastrophic scenarios is discussed and potential avenues for the improvement of model accuracy are set forth.

5.1 GLM related limitations and improvements

Input data:

The Input datasets for fitting the GLM were carefully selected, and each represent a highly significant influence factor as was confirmed by the model results. The high resolution of five arcminutes was chosen to sufficiently capture the heterogeneity of agricultural production. However, the high resolution, the spatial nature, and the specifics of the data lead to numerous challenges. First and foremost, the datasets do not actually showcase the real distribution of the specific variables but rather a statistical approximation of the real distribution. Spatial downsampling techniques introduce high levels of uncertainty into the dataset which are consequently replicated in the analysis at hand. Uncertainty itself is inevitable in modelling, however, modelling based on multiple different datasets leads to multiple types of uncertainty shaping the model. The datasets used in this analysis

were not harmonized against each other and standardization was only exercised by some on the country level against FAOSTAT data. In consequence the layers do not necessarily align: they differ in the extent covered and in the spatial distribution of the values. Discrepancies in the extent result in missing data points in the combined dataset used in the analysis. Especially the variables mechanized and pesticides covered substantially less cells than the remaining layers. Due to a lack of reliable data on explaining variables to estimate the missing values for either factor and the number of missing points being too large for less sophisticated interpolation methods, the rows containing missing values were dropped. The dropped values coincide for the most part with cells containing small areas of the respective crop as can be seen in

Figure 6. The grey areas represent the cells which contain cropland for the specific crop but were excluded from the analysis. By far the largest number of the excluded cells contain less than 100 ha of harvested crop area. Hence, even though many cells were dropped before calibrating the model, the remaining data still represent the main growing regions for each crop. The second consequence of malalignment between input datasets has more severe effects on the model accuracy. If the spatial distribution of the values does not align across datasets the underlying relationship between dependent and independent variables, which constitutes the very subject of the analysis, is possibly misrepresented. This effect can be observed in the characteristics of the outliers of each individual dataset, depicted in Table 5. According to what is known about the relationship between yield and agricultural inputs, it is expected that high yields coincide with high values for the explaining variables. In terms of the outliers, it would be anticipated that most outliers lie in the same cell: e.g., if six datasets each contain five outliers, the expected number of affected cells would also be five and not thirty. Table 5, however, shows that the number of cells containing outliers is almost as high the total number of outlier values because the highest value found in the N fertilizer dataset does not pertain to the same grid cell as the highest value for yield. The outliers are another result of the special characteristics of the input datasets. As described in chapter 3 all values above the 99.9^{th} percentile were considered as outliers. This distinction was made because all continuous input datasets contained unusually high values which were unrealistic like yields of 60 t/ha and N fertilizer application rates of more than 4 t/ha. The exceptional nature of these data points is illustrated by comparing the

mean of the outliers with the mean of the remaining cells: in most cases it is at least four times, in many cases ten times higher. Even though there is reason to assume that more values on both ends of the scale, albeit feasible, can be attributed to calculation errors or relics of the downsampling approach this could not be validated and therefore, it was refrained from excluding more values.

Due to the spatial nature of the analyzed data the yield value in each cell does not simply represent one unit but is rather tied to the area in each cell where the crop is

Table 5: Characteristics of the 99.9th percentile outliers in each of the continuous input datasets and the combined nitrogen variable. For comparison the mean of the remaining data points is also computed. The last column shows the number of rows in the analysis dataset containing outliers and the sum of the count for each crop.

Crop	Variable	Count	Min (kg/ha)	Max (kg/ha)	Mean (kg/ha)	Mean of remaining cells (kg/ha)	total number of rows (outliers)
Maize	Yield	199	18,746	43,447	22,056	5,520	2,615 (2,937)
	N fertilizer	194	370	4,447	1532	115	
	P fertilizer	165	54	494	202	19	
	N Manure	1981	44	1,209	73	7	
	N combined	199	391	4,579	1,546	122	
	Pesticides	199	12	12.3	11.95	3.8	
Wheat	Yield	214	12,904	2,3011	14,873	2,929	2,901 (3,188)
	N fertilizer	199	352	385	365	83	
	P fertilizer	214	52	126	94	12	
	N Manure	2133	43	1,093	65	5.2	
	N combined	214	380	1,099	414	88	
	Pesticides	214	1.8	4	1.9	0.5	
Soybean	Yield	79	5,926	11,768	7,601	2,280	1,056 (1,178)
	N fertilizer	75	364	395	370	97	
	P fertilizer	76	51	57	53	21	
	N Manure	790	37	245	51	5.1	
	N combined	79	376	483	395	102	
	Pesticides	79	6.5	7	6.7	3.3	
Rice	Yield	96	16,087	52,018	22,649	4,051	1,271 (1,413)
	N fertilizer	82	395	4,447	939	119	
	P fertilizer	89	56	494	111	18	
	N Manure	954	35	642	57	5.2	
	N combined	96	397	4,447	871	124	
	Pesticides	96	10.8	12	11	2.3	

harvested. As a result, yield values in cells with large harvested areas have a higher importance for the overall crop yield production than values with smaller harvested areas. A standard GLM, however, attributes the same weight to each data point, assuming that each data point stands for one observation. This leads to yields in small areas having a disproportionately large influence on the model relative to the area they cover while yields on large areas carry proportionately less weight. To address this imbalance by narrowing the range of the harvested area values, cells containing less than 100 ha of harvested area were excluded from the modelling dataset.

Figure 6 depicts the spatial distribution of all cells not considered in the analysis in grey. Noticeably, a large portion of these cells is located in Africa. This coincides with the uncertainty reported by Yu et al. (2020) as they estimate that the uncertainty of the SPAM2010 dataset is highest in Africa. Apart from the cumulation in African countries, the dropped cells concentrate outside of the main growing regions for the respective crop. For rice and soybean this includes Europe and Central America and for rice also South America. Maize and wheat overall count with less and smaller clusters of excluded cells as both have major growing zones in most regions of the world.

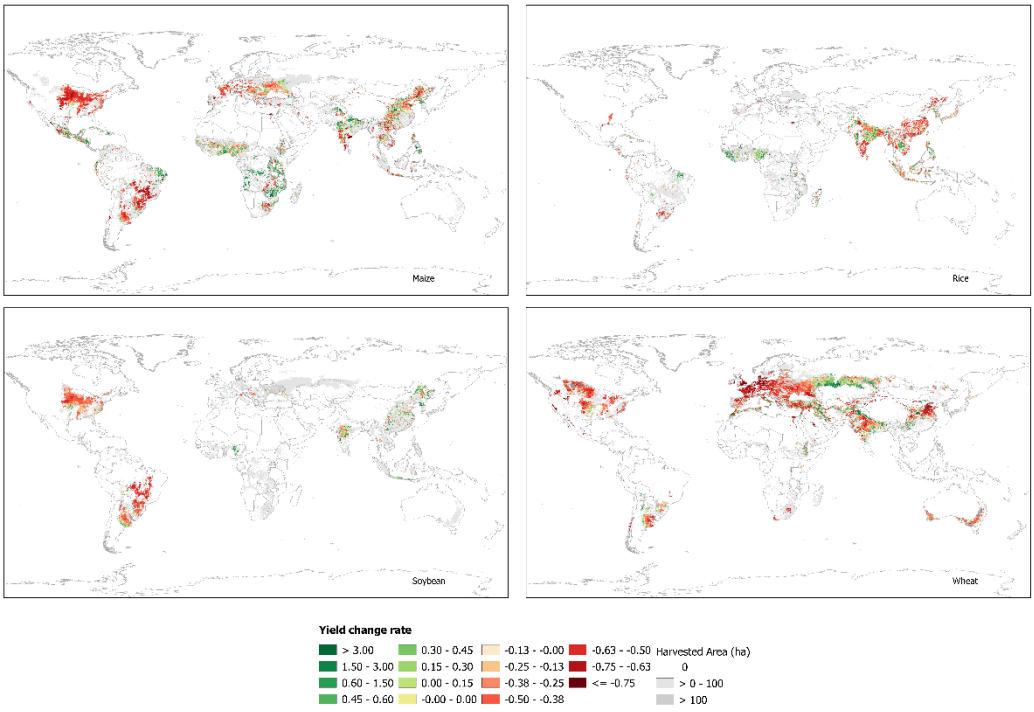

Figure 6: Yield change rate in phase 1 at 5 arcmin resolution. Harvested area for each crop.

Solely the maize GLM was calibrated on sufficient points for that region to yield viable results for most of the African continent.

Working with spatial data can also lead to effects of autocorrelation among data points. Autocorrelation refers to values being similar or the same due to geographic proximity. In high resolution datasets which are derived from statistical interpolation the effect is enhanced as more cells in close vicinity to each other tend to contain the same value. Considering that classical generalized linear models are not equipped to handle this relationship, autocorrelation can skew model results, especially in combination with misaligned data sets. As it is difficult to account for autocorrelation in a standard GLM, possible ways to address it are discussed in the next section about the methodological approach.

Methodological approach:

The modelling of crop growth and crop yields has a long history and extensive literature on crop modelling approaches exist (for an overview see Van Ittersum and Donatelli 2003). Generally, climate impacts on crop yields are assessed by using process-base models (Olesen and Bindi 2002, Easterling et al. 2007) and there has been a work on estimating the effects of a nuclear winter scenario with a DSSAT model (Xia and Robock, 2013). Process-based crop models simulate the physical plant growth of a crop in great detail. However, these models are not very well suited for the use case presented in this work. Firstly, calibrating and running the models is too time consuming and data intensive for a first assessment and therefore, beyond the scope of the work. Furthermore, the crop models are currently not well adapted to the requirements of the analysis at hand as management techniques and pesticide influences are sparsely implemented. As presented in chapter 4, both aspects are crucial for the investigation of LoI impacts on crop yields. A second approach is the modelling of effects based on empirical relationships between yield and the explaining variables as reported in the literature. This method, however, does not allow for the level of spatial detail sought in assessment. Multiple regression or generalized linear models were considered as the third alternative. Statistical regression models have previously been applied to assess factors that influence spatial variability in observed yield (Bakker et al. 2005, Kaufmann and Snell 1997, Reidsman et al. 2007) and in predictive crop modelling contexts (Ferraro et al. 2009). The approach was chosen as the best fit for the proposed use case.

The GLM approach provided good results for a first spatial estimate. Nonetheless, as discussed above, there is room to improve the fit of the GLM beyond the scope of this thesis. Several limitations are listed above, namely the misalignment of the spatial value distribution between datasets, the differing weight of each yield value according to the harvested area and autocorrelation between values in close vicinity. All these aspects can be addressed by applying special forms of the regression model. A weighted regression can be employed to ensure that each yield value is included into the model according to the size of the harvested area in the same cell. The same concept is useful to handle autocorrelation in the data. In a geographically weighted regression, the cells are weighted according to their proximity. The implementation is more difficult, however, as the calculation of the weights is more complex. The confounding effect of misaligned data can be eased in two different ways. First a different resolution can be chosen, either by choosing coarser input datasets or by upsampling the high-resolution datasets. Upsampling can smooth out misaligned cells to some degree by averaging over a larger cell area. The datasets with a coarser resolution might not have the level of uncertainty to begin with. Ideally, datasets are retrieved from one source. In the use case at hand a country-level analysis could be sensible as most of the variables can be obtained from the FAOSTAT database. Apart from managing the resolution, the fuzzy regression is a good tool to correct for high variability and mismatch in the data. Huang et al. (2010) recommend the application of soft computing like fuzzy regression for agricultural predictions as real-world data tends to be too imprecise to be analyzed with hard computing methods. In contrast to “hard” methods like a regular GLM, fuzzy logic does not decide between true and false but rather estimates the degree of truth for a value. Based on this logic it is better equipped to handle imprecise relationships and confounding factors.

Next to the numerous special regression forms, accounting for missing variables is another method to improve model accuracy. Missing variables can be additional explaining factors but also interactions between already included variables. The present model does not include interactions. The categorical variables were coded as dummies to be considered in the GLM, but this type of codification does not allow for a correct fitting of the interactions. Instead, effect coding must be applied.

5.2 LoI prediction related limitations, improvements, and aspects

The results demonstrate a substantial difference between phase 1 and phase 2 yield losses. It shows that phase 1 can be critical in the preparation for phase 2 because the yield losses are still manageable in first phase. This can provide the time necessary to adapt to the new circumstances by building up non-electrical logistic infrastructure, building tools and wagons, establish a communication system, implement new farming techniques, and crop rotations to manage pests and nutrients and just overall adjust as a society. The crucial component is the continued use of the agricultural machinery as it ensures that tasks can be completed on large farms even if the preparations for the transition to a human and animal operated system are still underway. In comparison to nutrient and pesticide inputs, irrigation and mechanized have a large effect size for all crops. However, this is probably due to the relationship between those two variables and the dependent variable which is clearer cut than for the remaining continuous variables. Potentially the effect sizes in the models are also influenced by missing variable bias. Due to data unavailability some of the factors that were identified as important for estimating yields in a LoI scenario were not included in the GLM and there could be components which are not yet known to influence the crop yield.

The following elements were not accounted for in the analysis: seed availability, (dominant) variety and knowledge of farmers. Beyond these potential model input factors, there are other characteristics of a LoI scenario which codetermine the availability of the input variables in case of a catastrophe. The characteristics considered in the model are specified in chapter 3. Additionally, influences can result from the availability of feed for draft animals and tools and materials for draft work, draft animals' constitution, population relocation, climate change, alternative pest control methods, crop rotations, alternative nutrient sources, means to conserve food and the time it takes to slaughter an animal. All listed factors and aspects have the potential to improve or decrease the crop yield in a LoI scenario. Nonetheless, most are likely to worsen the catastrophic impact. The two most important factors are:

- Seed availability,
- (dominant) variety

Seed availability and the distribution of crop varieties are closely interlinked. A large share of farmers, especially in industrialized countries, purchase their seeds from large global companies and do not retain seeds from their own harvest for the next year. Oftentimes these varieties are specifically bred to grow well in high-input conditions, some are even resistant against certain pesticides, and to be bought again. This does not mean that these seeds will not grow, nor will they necessarily grow badly under low input conditions, but they are certainly more prone to crop failure than local land races. In a global failure of electrical infrastructure highly specialized and industrialized plant breeding and seed production will likely also be disrupted. Maize would be particularly strongly affected as almost all maize crops are grown from hybrid seeds which are inbred varieties targeted specifically at a high one-year performance. If there are no seeds available from large seed companies and the seeds saved from the high-yielding varieties do not perform well in the LoI scenario, there will not be sufficient seed from landraces available to cultivate all the current cropland area.

6 Conclusion

This thesis work was able to provide new insights on the impact of a large-scale industrial outage triggered by a global catastrophe on the yields of maize, rice, soybean, and wheat. The first spatially explicit and crop specific estimate for the effect on crop yields is presented for two phases of a LoI scenario differing in severity.

Based on the maps presented at five arcmin resolution, it can be concluded that the spatial dimension of the repercussions of the catastrophe is highly relevant. A clear distinction between strongly and barely affected regions is visible in the data. The identified hotspots varied between crops according to the main growing regions but overall aligned with strongly industrialized agriculture.

Noticeable differences could also be registered between phase 1 and 2. Available stocks of agricultural inputs, albeit constituting only a fraction of current use, substantially lessened the yield losses. Phase 1 is therefore a crucial step to allow agriculture to adapt to the new conditions.

The elected methodological approach proved suitable for the use case in this thesis. The fitted GLMs showed good agreement with the data (ρ^2 between 0.34 and 0.47) and all chosen variables had a significant effect on the crop yield ($p < 0.05$). The models provide a solid basis to further develop the statistical approach by including more relevant variables or applying specific variants of the regression methodology.

Proceeding from these conclusions further research should focus on specifying the estimates by developing the statistical approach presented here or by combining a statistical framework with either a machine learning approach or a process-based crop model. The methodology could also be applied to a wider crop range to gauge which crops fare better under losing industry conditions. In addition, a regional focused analysis could provide valuable insights. Improving the understanding of the dynamics in hotspot regions is one major goal while an analysis in Africa is advisable due to the lack of coverage in the work at hand.

COVID-19 has illustrated the unexpected urgency of a global catastrophe and how fast things can go south. Let this work be a reason to be hopeful, that next time, we'll do better.

7 References

ALLFED (2021, October 18). *Home - ALLFED*. https://allfed.info

Alston, J. M., & Pardey, P. G. (2014). Agriculture in the Global Economy. *Journal of Economic Perspectives*, *28*(1), 121–146. https://doi.org/10.1257/jep.28.1.121

Avin, S., Wintle, B. C., Weitzdörfer, J., Ó hÉigeartaigh, S. S., Sutherland, W. J., & Rees, M. J. (2018). Classifying global catastrophic risks. *Futures*, *102*, 20–26. https://doi.org/10.1016/j.futures.2018.02.001

Bakker, M.M., Govers, G., Ewert, F., Rounsevell, M., Jones, R. (2005). Variability in regional wheat yields as a function of climate, soil and economic variables: assessing the risk of confounding. *Agriculture, Ecosystems and Environment*, *110*(3-4), 195–209.

Baum, S., & Barrett, A. (2017). Global Catastrophes: The Most Extreme Risks. In V. Bier (Ed.), *Risk in Extreme Environments: Preparing, Avoiding, Mitigating, and Managing* (pp. 174–184). New York: Routledge. https://ssrn.com/abstract=3046668

Baum, S. D., Denkenberger, D. C., Pearce, J. M., Robock, A., & Winkler, R. (2015). Resilience to global food supply catastrophes. *Environment Systems and Decisions*, *35*(2), 301–313. https://doi.org/10.1007/s10669-015-9549-2

Bostrom, N., & Ćirković, M. M. (Eds.) (2008a). *Global catastrophic risks*. Oxford: Oxford University Press.

Bostrom, N., & Ćirković, M. M. (2008b). Introduction. In N. Bostrom & M. M. Ćirković (Eds.), *Global catastrophic risks* (pp. 1–30). Oxford: Oxford University Press.

Branco, P. A. B. (2020). *Food Production and Agriculture*. Ashland: Delve Publishing. https://ebookcentral.proquest.com/lib/kxp/detail.action?docID=5989639

Brozus, L., & Stiftung Wissenschaft und Politik (2020). *Preparing for the crises after COVID-19*. German Institute for International and Security Affairs. https://doi.org/10.18449/2020C51

Coates, J. F. (2009). Risks and threats to civilization, humankind, and the earth. *Futures*, *41*(10), 694–705. https://doi.org/10.1016/j.futures.2009.07.010

Cole, D., Denkenberger, D. C., Griswold, M., Abdelkhaliq, M., & Pearce, J. M. (2016). Feeding Everyone if Industry is Disabled. In International Disaster and Risk Conference (Chair), *IDRC DAVOS 2016 Integrative Risk Management - Towards Resilient Cities*, Davos. https://hal.archives-ouvertes.fr/hal-02113486

Cooper, C., & Sovacool, B. K. (2011). Not Your Father's Y2K: Preparing the North American Power Grid for the Perfect Solar Storm. *The Electricity Journal*, *24*(4), 47–61. https://doi.org/10.1016/j.tej.2011.04.005

Cutler, D. M., & Summers, L. H. (2020). The COVID-19 Pandemic and the $16 Trillion Virus. *JAMA*, *324*(15), 1495–1496. https://doi.org/10.1001/jama.2020.19759

Dempewolf, H., Eastwood, R. J., Guarino, L., Khoury, C. K., Müller, J. V., & Toll, J. (2014). Adapting Agriculture to Climate Change: A Global Initiative to Collect, Conserve, and Use Crop Wild Relatives. *Agroecology and Sustainable Food Systems*, *38*(4), 369–377. https://doi.org/10.1080/21683565.2013.870629

Denkenberger, D. C., & Pearce, J. M. (2014). *Feeding everyone no matter what: Managing food security after global catastrophe*. London: Academic Press. http://www.sciencedirect.com/science/book/9780128044476

Easterling, W.E., Aggarwal, P.K., Batima, P., Brander, K.M., Erda, L., Howden, S.M., Kirilenko, A., Morton, J., Soussana, J.-F., Schmidhuber, J., Tubiello, F.N., 2007. Food, fibre and forest products. In: Parry, M.L., Canziani, O.F., Palutikof, J.P., van der Linden, P.J., Hanson, C.E. (Eds.), *Climate Change 2007: Impacts Adaptation and Vulnerability. Contribution of Working Group II to the Fourth Assessment Report of the Intergovernmental Panel on Climate Change* (pp. 273–313). Cambridge, UK: Cambridge University Press.

Electrical Engineering Portal (2013, December 30). *Large power transformer tailored to customers' specifications*. https://electrical-engineering-portal.com/an-overview-of-large-power-transformer-lpt

Evenson, R. E., & Gollin, D. (2003). Assessing the impact of the green revolution, 1960 to 2000. *Science*, *300*(5620), 758–762. https://doi.org/10.1126/science.1078710

FAOSTAT (2021a, September 15). *Crops and livestock products.* https://www.fao.org/faostat/en/#data/QCL

FAOSTAT (2021b, July 19). *Pesticide Use*. https://www.fao.org/faostat/en/#data/RP

Ferraro, D. O., Rivero, D. E., Ghersa, C. M. (2009). An analysis of the factors that influence sugarcane yield in Northern Argentina using classification and regression trees. *Field Crops Research*, *112*(2-3), 149-157. https://doi.org/10.1016/j.fcr.2009.02.014

Fischer, G., Nachtergaele, F., van Velthuizen, H., Chiozza, F., Franceschini, G., Henry, M., Tramberend, S. (2021). *Global Agroecological Zones v4 (GAEZ v4): Model Documentation*. Rome: FAO. https://doi.org/10.4060/cb4744en

Flynn, K. (1999). *Overview of public health and urban agriculture: water, soil and crop contamination and emerging urban zoonoses*. International Development Research Centre (IDRC): https://idl-bnc-idrc.dspacedirect.org/bitstream/handle/10625/32952/117784.pdf?sequence=5

Food and Agriculture Organization of the United Nations (2017). *World fertilizer trends and outlooks to 2020*. Rome.

Goldin, I., & Vogel, T. (2010). Global Governance and Systemic Risk in the 21st Century: Lessons from the Financial Crisis. *Global Policy*, *1*(1), 4–15. https://doi.org/10.1111/j.1758-5899.2009.00011.x

Hartman, G. L., West, E. D., & Herman, T. K. (2011). Crops that feed the World 2. Soybean—Worldwide production, use, and constraints caused by pathogens and pests. *Food Security*, *3*(1), 5–17. https://doi.org/10.1007/s12571-010-0108-x

Hayakawa, H., Ebihara, Y., Willis, D. M., Toriumi, S., Iju, T., Hattori, K., Knipp, D. J. (2019). Temporal and Spatial Evolutions of a Large Sunspot Group and Great Auroral Storms Around the Carrington Event in 1859. *Space Weather*, *17*(11), 1553–1569. https://doi.org/10.1029/2019SW002269

Helbing, D. (2013). Globally networked risks and how to respond. *Nature*, *497*(7447), 51–59. https://doi.org/10.1038/nature12047

Huang, Y., Lan, Y., Thomson, S. J., Fang, A., Hoffmann, W. C. (2010). Development of soft computing and applications in agricultural and biological engineering. *Computers and Electronics in Agriculture*, *71*(2), 107-127. https://doi.org/10.1016/j.compag.2010.01.001

Kassam, A., Friedrich, T., & Derpsch, R. (2019). Global spread of Conservation Agriculture. *International Journal of Environmental Studies*, *76*(1), 29–51. https://doi.org/10.1080/00207233.2018.1494927

Kaufmann, R.K., Snell, S.E. (1997). A biophysical model of corn yield: integrating climatic and social determinants. *American Journal of Agricultural Economics*, *79*(1), 178–190.

Kopittke, P. M., Menzies, N. W., Wang, P., McKenna, B. A., & Lombi, E. (2019). Soil and the intensification of agriculture for global food security. *Environment International*, *132*, 105078. https://doi.org/10.1016/j.envint.2019.105078

Lee, L. K., & Nielsen, E. G. (1987). The extent and costs of groundwater contamination by agriculture. *Journal of Soil and Water Conservation*, *42*(4), 243–248. https://www.jswconline.org/content/42/4/243.short

Lenzen, M., Li, M., Malik, A., Pomponi, F., Sun, Y.-Y., Wiedmann, T., ? Yousefzadeh, M. (2020). Global socio-economic losses and environmental gains from the Coronavirus pandemic. *PLOS ONE*, *15*(7). https://doi.org/10.1371/journal.pone.0235654

Liu, H.-Y., Lauta, K., & Maas, M. (2020). Apocalypse Now? *Journal of International Humanitarian Legal Studies*, *11*(2), 295–310. https://doi.org/10.1163/18781527-01102004

Lu, C., & Tian, H. (2016). *Half-degree gridded nitrogen and phosphorus fertilizer use for global agriculture production during 1900-2013.* https://doi.org/10.1594/PANGAEA.863323

Lu, C., & Tian, H. (2017). Global nitrogen and phosphorus fertilizer use for agriculture production in the past half century: shifted hot spots and nutrient imbalance. *Earth System Science Data*, *9*(1), 181–192. https://doi.org/10.5194/essd-9-181-2017

Maggi, F., Tang, F., La Cecilia, D., & McBratney, A. (2020). *Global Pesticide Grids (PEST-CHEMGRIDS), Version 1.01*. Palisades, NY: NASA Socioeconomic Data and Applications Center (SEDAC). https://doi.org/10.7927/WEQ9-PV30

Maggi, F., Tang, F. H. M., La Cecilia, D., & McBratney, A. (2019). Pest-CHEMGRIDS, global gridded maps of the top 20 crop-specific pesticide

application rates from 2015 to 2025. *Scientific Data*, *6*(1), 170. https://doi.org/10.1038/s41597-019-0169-4

Maher, T., & Baum, S. (2013). Adaptation to and Recovery from Global Catastrophe. *Sustainability*, *5*(4), 1461–1479. https://doi.org/10.3390/su5041461

Manheim, D. (2020). The Fragile World Hypothesis: Complexity, Fragility, and Systemic Existential Risk. *Futures*, *122*, 102570. https://doi.org/10.1016/j.futures.2020.102570

McFadden, D. (1977). Quantitative Methods for Analyzing Travel Behaviour of Individuals: Some Recent Developments. *Cowles Foundation Discussion Papers*. (474). https://ideas.repec.org/p/cwl/cwldpp/474.html

Mekhaldi, F., Muscheler, R., Adolphi, F., Aldahan, A., Beer, J., McConnell, J. R., Woodruff, T. E. (2015). Multiradionuclide evidence for the solar origin of the cosmic-ray events of AD 774/5 and 993/4. *Nature Communications*, *6*(1), 8611. https://doi.org/10.1038/ncomms9611

Miedaner, T. (2005). *Von der Hacke bis zur Gen-Technik: Kulturgeschichte der Pflanzenproduktion in Mitteleuropa* (1. Aufl.). Frankfurt am Main: DLG-Verl.

Myers, S. S., Smith, M. R., Guth, S., Golden, C. D., Vaitla, B., Mueller, N. D., Huybers, P. (2017). Climate Change and Global Food Systems: Potential Impacts on Food Security and Undernutrition. *Annual Review of Public Health*, *38*, 259–277. https://doi.org/10.1146/annurev-publhealth-031816-044356

Naeem, M., Ansari, A. A., & Gill, S. S. (2020). *Contaminants in Agriculture*. Cham: Springer International Publishing. https://doi.org/10.1007/978-3-030-41552-5

National Science & Technology Council (2019). *National Space Weather Strategy and Action Plan.* https://trumpwhitehouse.archives.gov/wp-content/uploads/2019/03/National-Space-Weather-Strategy-and-Action-Plan-2019.pdf

Neff, R. A., Parker, C. L., Kirschenmann, F. L., Tinch, J., & Lawrence, R. S. (2011). Peak oil, food systems, and public health. *American Journal of Public Health*, *101*(9), 1587–1597. https://doi.org/10.2105/AJPH.2011.300123

Neumann, K., Verburg, P., Stehfest, E., & Müller, C. (2010). The yield gap of global grain production: A spatial analysis. *Agricultural Systems 103(5).* 316-326. https://doi.org/10.1016/J.AGSY.2010.02.004

North American Electric Reliability Corporation, & U.S. Department of Energy (2010, October). *High-Impact, Low-Frequency Event Risk to the North American Bulk Power System*. https://energy.gov/sites/prod/files/High-Impact%20Low-Frequency%20Event%20Risk%20to%20the%20North%20American%20Bulk%20Power%20System%20-%202010.pdf

Olesen, J.E., Bindi, M. (2002). Consequences of climate change for European agricultural productivity, land use and policy. *European Journal of Agronomy 16*(4), 239–262.

Office of Electricity Delivery and Energy Reliability (04.2014). *Large power transformers and the U.S. electrical grid*. Retrieved from https://energy.gov/sites/prod/files/2014/04/f15/LPTStudyUpdate-040914.pdf

Park, C.-Y., Villafuerte, J., Abiad, A., Narayanan, B., Banzon, E., Samson, J., Tayag, M. C. (2020). An Updated Assessment of the Economic Impact of COVID-19. *ADB Briefs 133*. https://doi.org/10.22617/BRF200144-2

Porwollik, V., Rolinski, S., Heinke, J., & Müller, C. (2019). Generating a rule-based global gridded tillage dataset. *Earth System Science Data*, *11*(2), 823–843. https://doi.org/10.5194/essd-11-823-2019

Porwollik, V., Rolinski, S., & Müller, C. (2019). *A global gridded data set on tillage (V. 1.1)*. [Data set] GFZ Data Services. https://doi.org/10.5880/PIK.2019.009

Prak, M. R. (Ed.) (2006). *Early modern capitalism: Economic and social change in Europe, 1400 - 1800*. London: Routledge.

Rabbinge, R. (1993). The ecological background of food production. *Crop Protection and Sustainable Agriculture. Ciba Found. Symp. 177, John Wiley & Sons, Chicester*, 2–29. https://research.wur.nl/en/publications/the-ecological-background-of-food-production

Reidsma, P., Ewert, F., Oude Lansink, A. (2007). Analysis of farm performance in Europe under different climate and management conditions to improve understanding of adaptive capacity. *Climatic Change 84*(3), 403–422.

Ritchie, H., & Roser, M. (2013). *Crop Yields*. Our World in Data. https://ourworldindata.org/crop-yields

Rivers, M. (2021). *Methodology for a global gridded dataset on irrigation reliant on electricity at five arminutes resolution*. Retrieved from https://github.com/allfed/ImportReliantIrrigation

Sánchez-Bayo, F., & Wyckhuys, K. A. (2019). Worldwide decline of the entomofauna: A review of its drivers. *Biological Conservation*, *232*, 8–27. https://doi.org/10.1016/j.biocon.2019.01.020

Sandberg, A. (2018). Human Extinction from Natural Hazard Events. *Oxford Research Encyclopedia of Natural Hazard Science*. https://doi.org/10.1093/acrefore/9780199389407.013.293

Schieb, P.-A., & Gibson, A. (2011). Geomagnetic Storms. *IFP/WKP/FGS(2011)4*

Seck, P. A., Diagne, A., Mohanty, S., & Wopereis, M. C. S. (2012). Crops that feed the world 7: Rice. *Food Security*, *4*(1), 7–24. https://doi.org/10.1007/s12571-012-0168-1

Shiferaw, B., Prasanna, B. M., Hellin, J., & Bänziger, M. (2011). Crops that feed the world 6. Past successes and future challenges to the role played by maize in global food security. *Food Security*, *3*(3), 307–327. https://doi.org/10.1007/s12571-011-0140-5

Shiferaw, B., Smale, M., Braun, H.-J., Duveiller, E., Reynolds, M., & Muricho, G. (2013). Crops that feed the world 10. Past successes and future challenges to the role played by wheat in global food security. *Food Security*, *5*(3), 291–317. https://doi.org/10.1007/s12571-013-0263-y

Siebert, S., Henrich, V., Frenken, K., & Burke, J. (2013). *Update of the Digital Global Map of Irrigation Areas (GMIA) to Version 5*. [Data set] https://doi.org/10.13140/2.1.2660.6728

Smil, V. (2017). *Energy and Civilization: A History*. Cambridge, London: The MIT Press.

Talib, M., & Mogotlhwane, T. M. (2011). Global Failure of ICT due to Solar Storm: A Worst Case Scenario Ahead. *Procedia Environmental Sciences*, *8*, 371–374. https://doi.org/10.1016/j.proenv.2011.10.058

United Nations Conference on Trade and Development (2021). Global economy could lose over $4 trillion due to COVID-19 impact on tourism | UNCTAD.

https://unctad.org/news/global-economy-could-lose-over-4-trillion-due-covid-19-impact-tourism

Van Ittersum, M., Donatelli, M. (Eds.). (2003). Modelling Cropping Systems: Science, Software and Applications [Special Issue]. *European Journal of Agronomy*, *18*(3-4).

Van Ittersum, M., Leffelaar, P., van Keulen, H., Kropff, M., Bastiaans, L., & Goudriaan, J. (2003). On approaches and applications of the Wageningen crop models. *European Journal of Agronomy*, *18*(3-4), 201–234. https://doi.org/10.1016/S1161-0301(02)00106-5

Van Ittersum, M. K., Cassman, K. G., Grassini, P., Wolf, J., Tittonell, P., & Hochman, Z. (2013). Yield gap analysis with local to global relevance—A review. *Field Crops Research*, *143*, 4–17. https://doi.org/10.1016/j.fcr.2012.09.009

Vermeulen, S. J., Campbell, B. M., & Ingram, J. S. (2012). Climate Change and Food Systems. *Annual Review of Environment and Resources*, *37*(1), 195–222. https://doi.org/10.1146/annurev-environ-020411-130608

Weiss, M., & Weiss, M. (2019). An assessment of threats to the American power grid. *Energy, Sustainability and Society*, *9*(1). https://doi.org/10.1186/s13705-019-0199-y

Wiener, J. B. (2016). The Tragedy of the Uncommons: On the Politics of Apocalypse. *Global Policy*, *7*, 67–80. https://doi.org/10.1111/1758-5899.12319

Wikipedia (2021). https://en.wikipedia.org/w/index.php?title=Stuxnet&oldid=1041792130

Wilson, C. (2008). *High Altitude Electromagnetic Pulse (HEMP) and High Power Microwave (HPM) Devices: Threat Assessments.*

World Bank (2021). Employment in agriculture (% of total employment) (modeled ILO estimate) [Data set]. https://data.worldbank.org/indicator/SL.AGR.EMPL.ZS

Xia, L., Robock, A. (2013). Impacts of a nuclear war in South Asia on rice production in Mainland China. *Climate Change*, *116*(2), 357-372. https://doi.org/10.1007/s10584-012-0475-8

Yu, Q., You, L., Wood-Sichra, U., Ru, Y., Joglekar, A. K. B., Fritz, S., Yang, P. (2020). A cultivated planet in 2010 – Part 2: The global gridded agricultural-

production maps. *Earth System Science Data*, *12*(4), 3545–3572. https://doi.org/10.5194/essd-12-3545-2020

Yudkowsky, E. (2008). Cognitive biases potentially affecting judgement of global risks. In N. Bostrom & M. M. Ćirković (Eds.), *Global catastrophic risks* (pp. 91–119). Oxford: Oxford University Press.

Zetter, K. (2016, January 20). Everything We Know About Ukraine's Power Plant Hack. *WIRED*. https://www.wired.com/2016/01/everything-we-know-about-ukraines-power-plant-hack/

Zhang, B., Tian, H., Lu, C., Dangal, S. R. S., Yang, J., & Pan, S. (2017a). Global manure nitrogen production and application in cropland during 1860–2014: a 5 arcmin gridded global dataset for Earth system modeling. *Earth System Science Data*, *9*(2), 667–678. https://doi.org/10.5194/essd-9-667-2017

Zhang, B., Tian, H., Lu, C., Dangal, S. R. S., Yang, J., & Pan, S. (2017b). *Manure nitrogen production and application in cropland and rangeland during 1860–2014: A 5-minute gridded global data set for Earth system modeling.* https://doi.org/10.1594/PANGAEA.871980b

Declaration of Originality

I confirm that the submitted thesis is original work and was written by me without further assistance. Appropriate credit has been given where reference has been made to the work of others.

The thesis was not examined before, nor has it been published. The submitted electronic version of the thesis matches the printed version.

Eidesstattliche Erklärung

Hiermit versichere ich, dass ich die von mir vorgelegte Masterarbeit

- selbständig verfasst habe,
- ich keine anderen als die in der Masterarbeit angegebenen Quellen und Hilfsmittelbenutzt habe,
- ich alle wörtlich oder sinngemäß aus anderen Werken übernommenen Inhalte als solche kenntlich gemacht habe.

Des Weiteren versichere ich, dass die von mir vorgelegte Masterarbeit weder vollständig noch in wesentlichen Teilen Gegenstand eines anderen Prüfungsverfahrens war oder ist.

Ich versichere zudem, dass die von mir eingereichte elektronische Version in Form und Inhalt der gedruckten Version der Masterarbeit entspricht.

Bad Wurzach, 23.10.2021 — Jessica Mörsdorf

Place, Date — Signature (Jessica Mörsdorf)